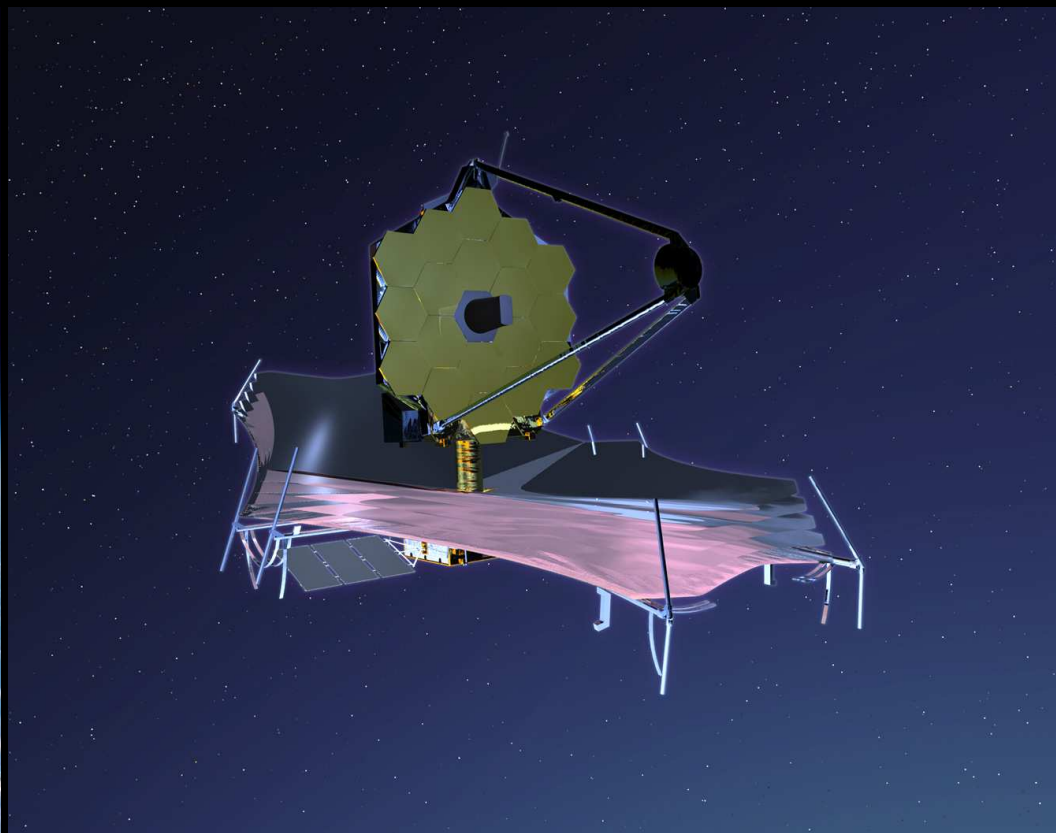


Constraints on weak AGN from HST FIGS data in the GOODS-North & GOODS-South Fields

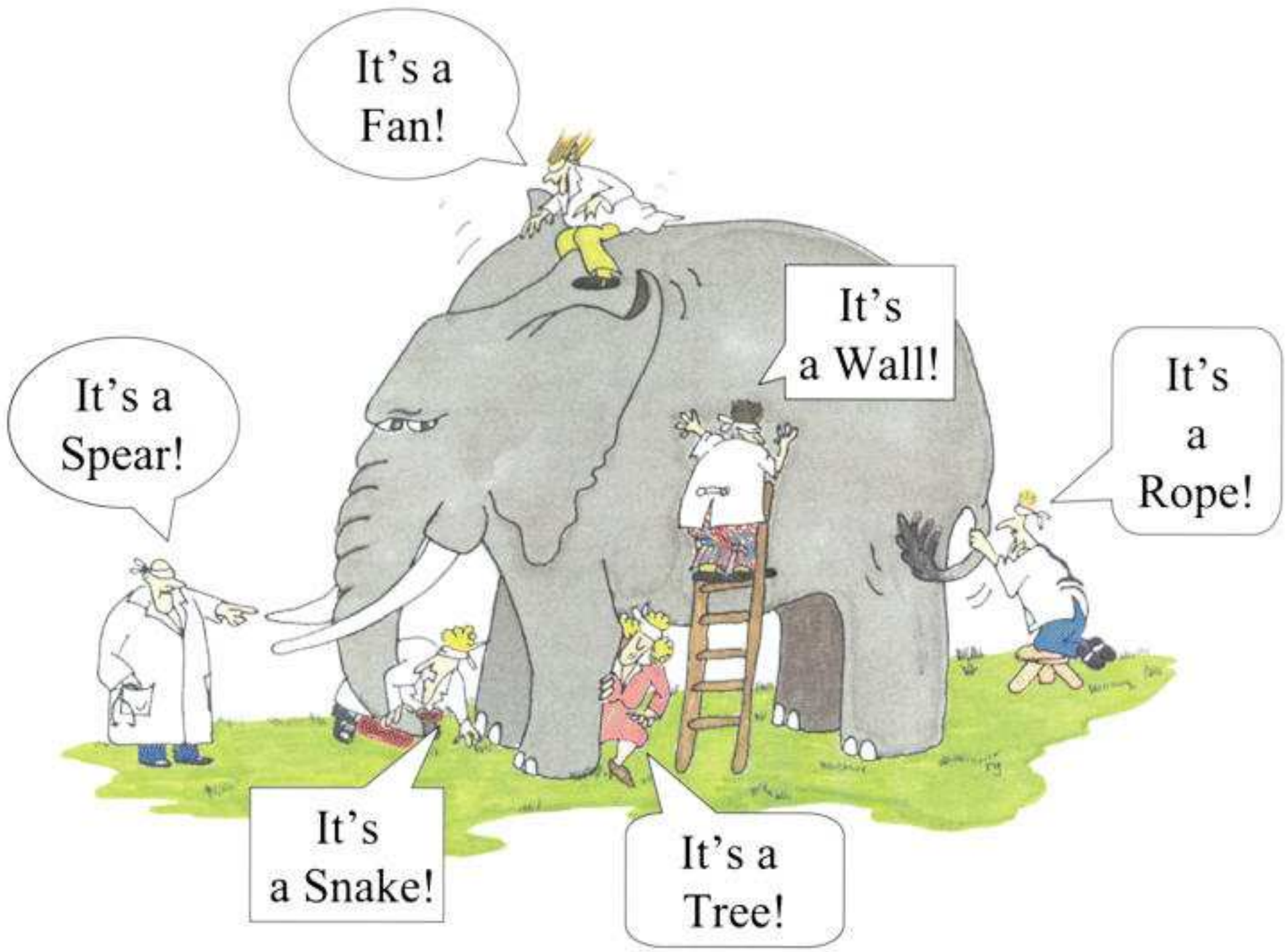
Rogier Windhorst, Bhavin Joshi (ASU) & Anton Koekemoer (STScI)



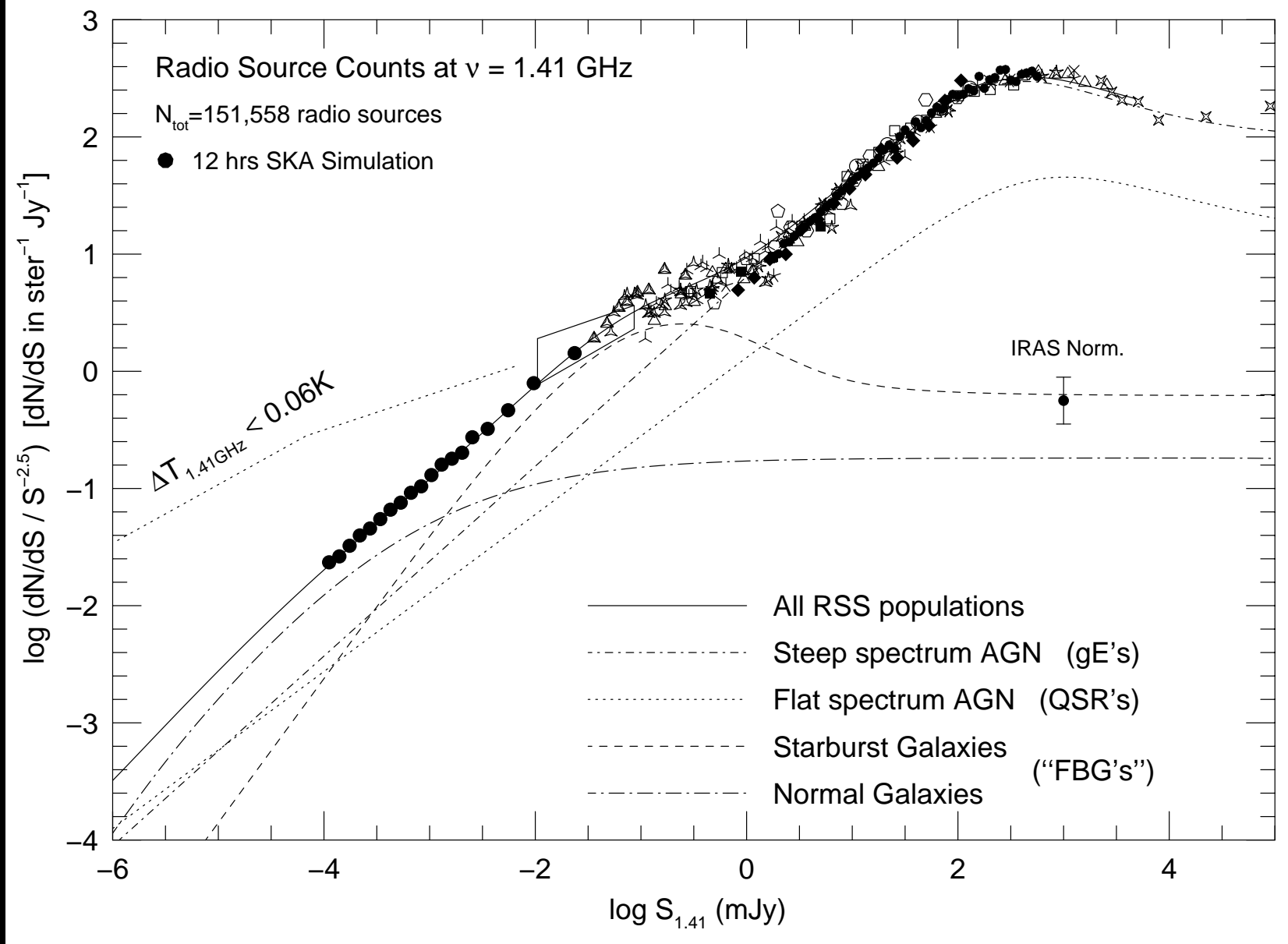
HST FIGS Telecon, Thursday Oct. 29, 2015

Outline

- (1) Weak AGN selection in GOODS-N+S & Summary of FIGS data.
- (2) SED ages of X-ray and Radio selected host galaxies vs. epoch:
Potential to trace weak AGN-growth vs. Galaxy Assembly.
- (3) Suggested Future Work on Weak AGN.
- (4) Summary and Conclusions.

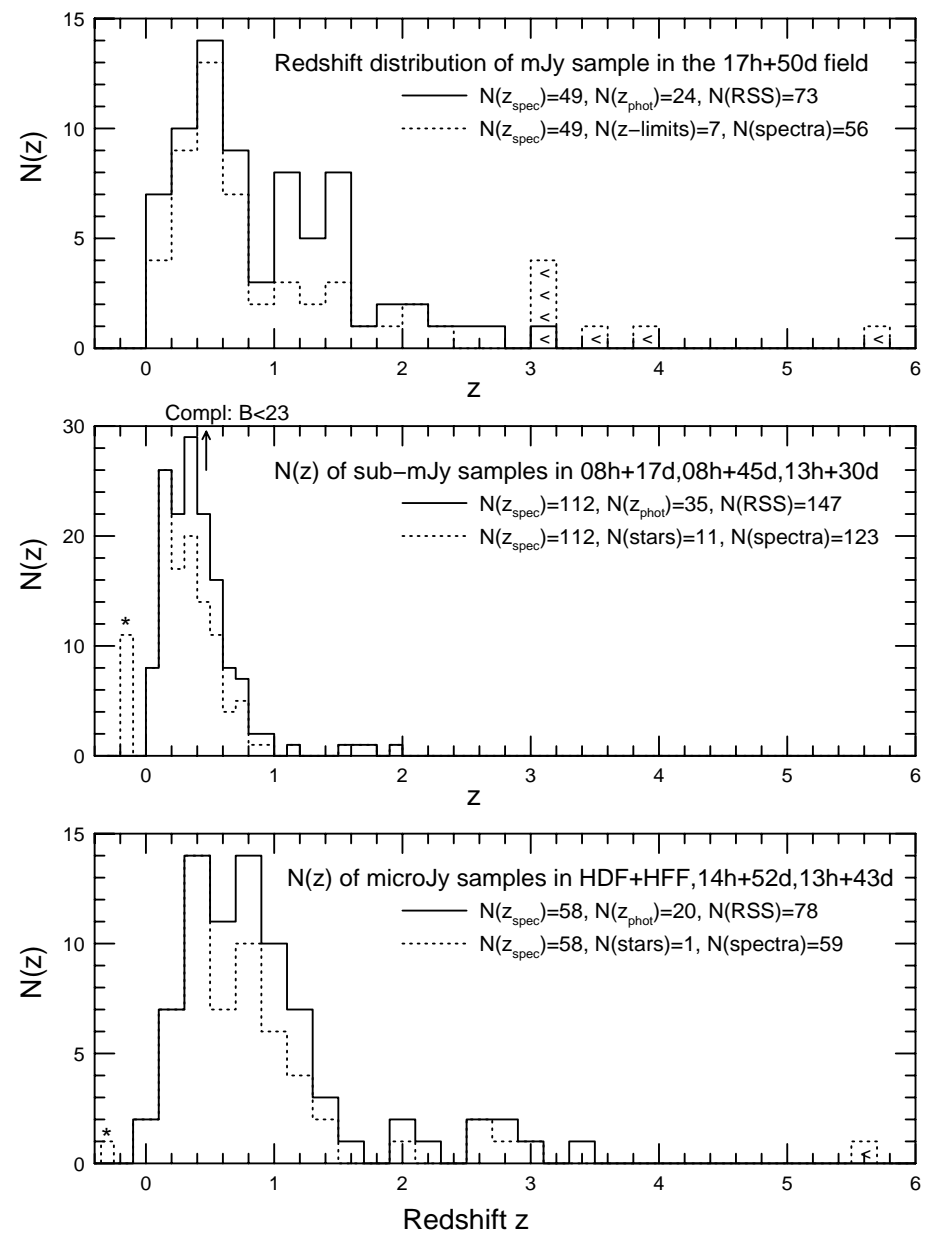
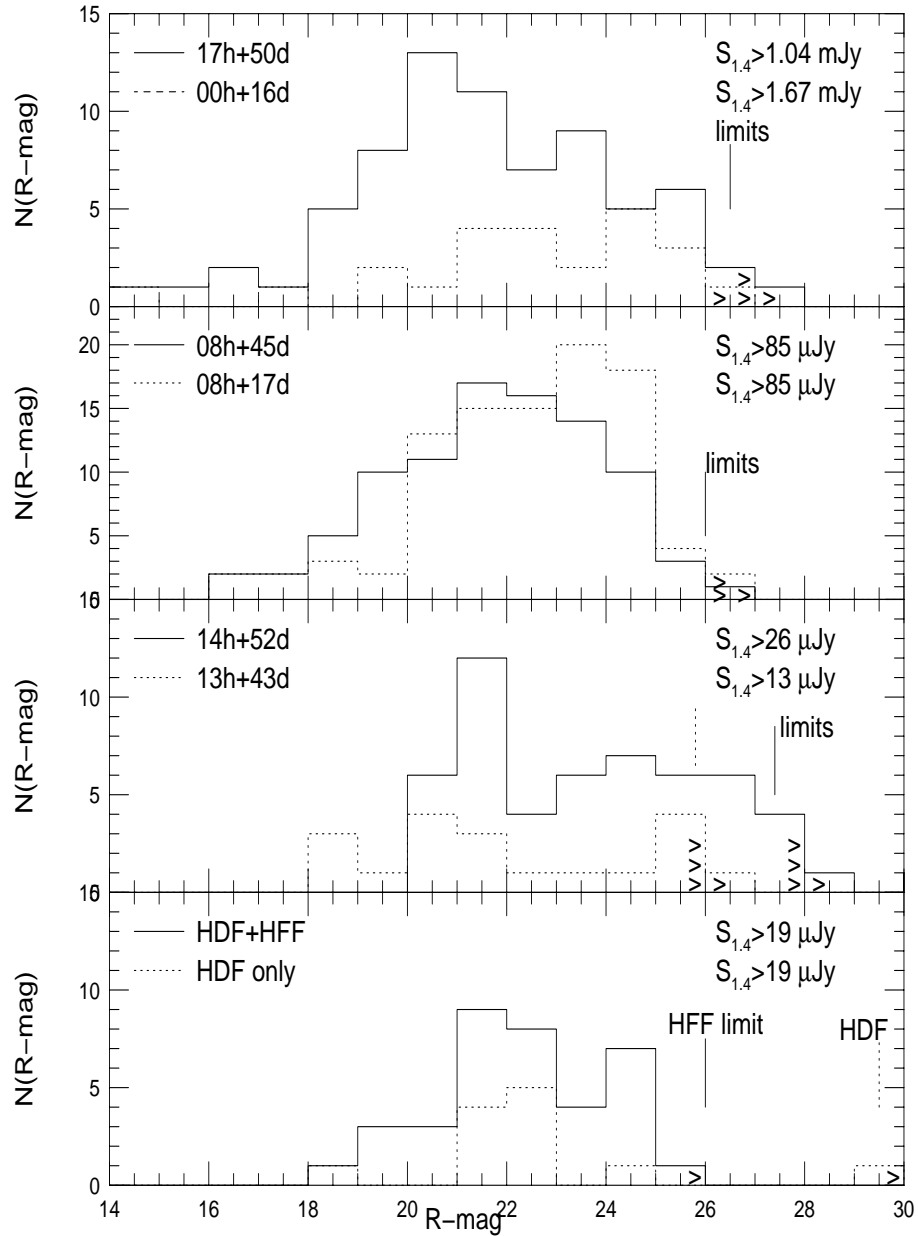


AGN are cosmic elephants that baffle both observers and theorists ... !



Norm. diff. 1.4 GHz source counts at $\mu\text{Jy} - \text{Jy}$ levels (Windhorst 2003):

- Steep+flat spectrum AGN (ellipticals+quasars) dominate at $S_{1.4} \gtrsim 1$ mJy.
- Starforming + normal spiral galaxies dominate counts at $S_{1.4} \lesssim 0.3$ mJy.
- About same in X-rays, but $f(\text{AGN}) \gg f(\text{X-ray binaries in starbursts})$.



Magnitude+redshift distributions of mJy and μ Jy samples (Windhorst 2003):

- Median R-band flux [Left] for mJy and μ Jy samples is $R \sim 22$ mag.
- Median redshift [Right] for mJy and μ Jy radio samples is $z \lesssim 0.8-1$.

Radio Sources with FIGS spectra

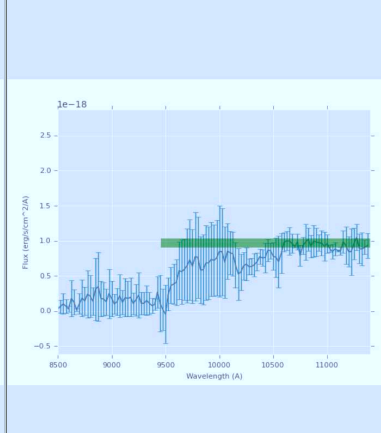
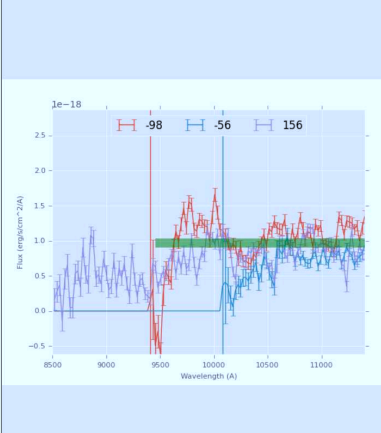
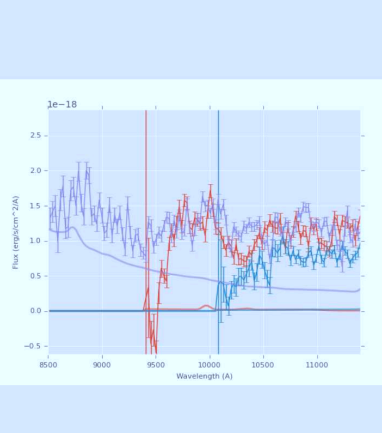
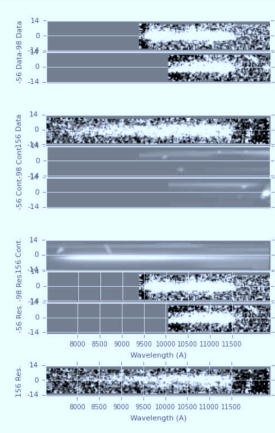
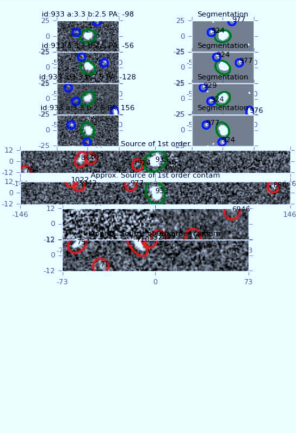
Reference	Fld	Instr. ν	5σ (μJy)	FWHM ($''$)	N_{FIGS}/N_{RSS}
Morrison ⁺ 2010 AJ, 188, 178	G-N	VLA 1.4GHz	20–40	17	11/37+10/31=21/68
Afonso ⁺ 2006 AJ, 131, 1216	G-S	ATCA 1.4GHz	70	17×7	1/9+1/2 = 2/11
Miller ⁺ 2013 ApJS, 205, 13	G-S	VLA 1.4GHz	30–35	3×2	3/20+10/23 = 13/43
TOTAL					36/122 (30%)

- Position error $\simeq 0.42 * \text{FWHM} / (S_p / \text{N-ratio})$.
 - FIGS spectra available for radio sources in $\sim 30\%$ of catalog search area.
- Following pages show all FIGS spectra in numerical order without filtering:

933

189.186813
62.310532
351.6750.0
(-141.4)
(257.0)

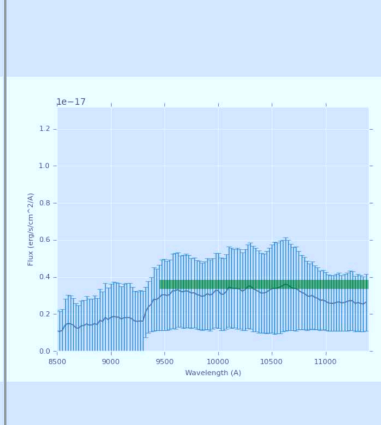
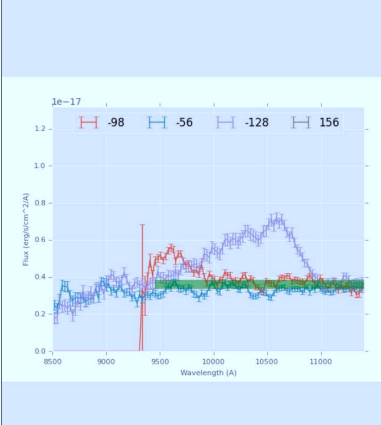
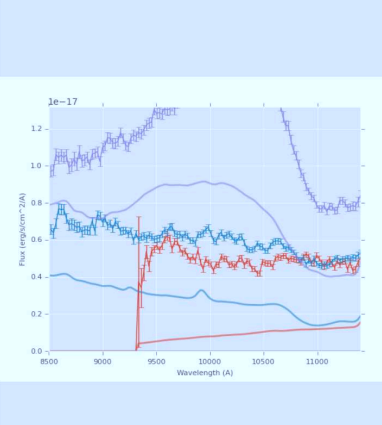
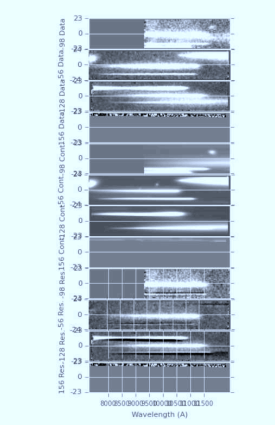
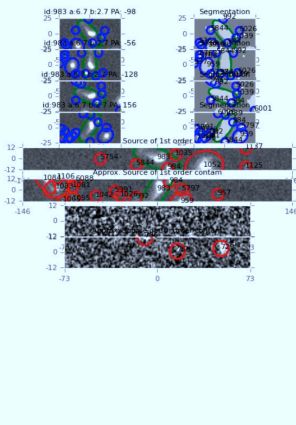
22.52



983

189.168900
62.309185
354.3986.8
(-138.7)
(493.8)

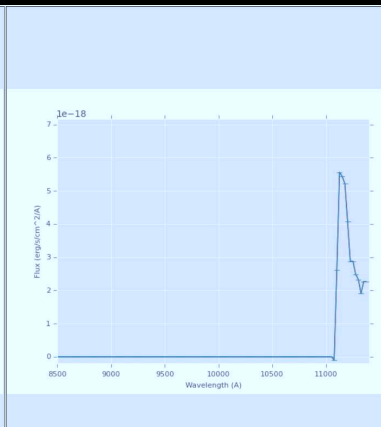
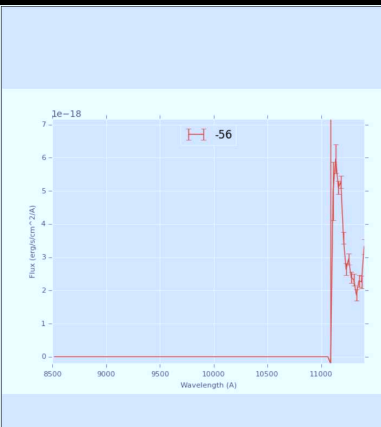
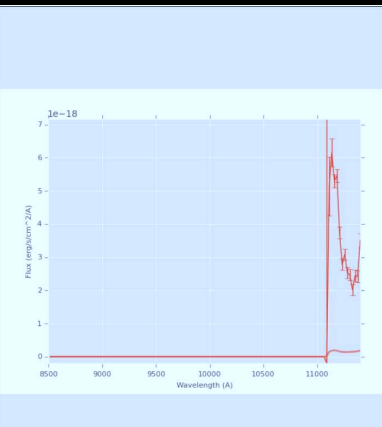
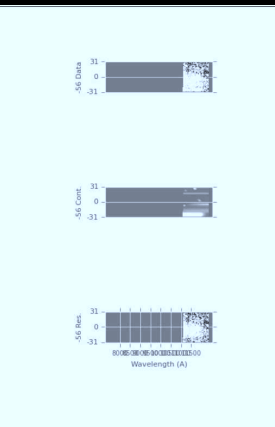
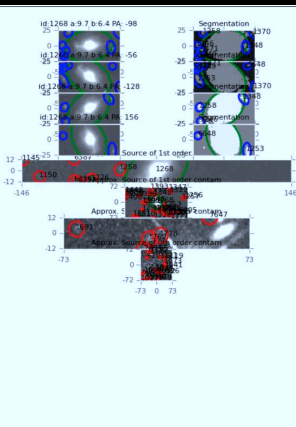
21.1



1268

189.220108
62.302135
267.5676.6
(-225.5)
(183.6)

18.77

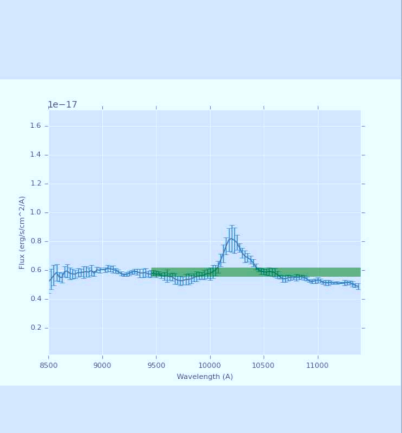
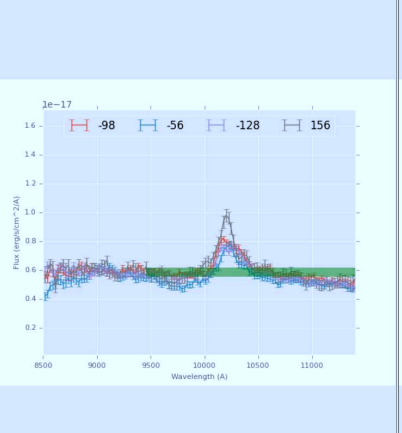
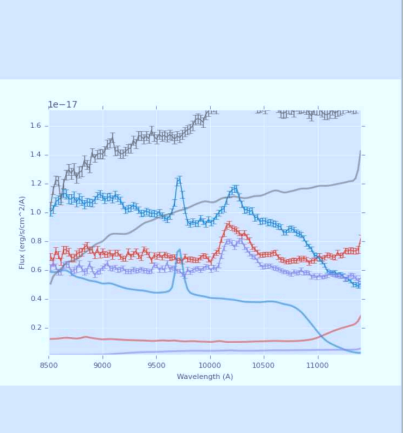
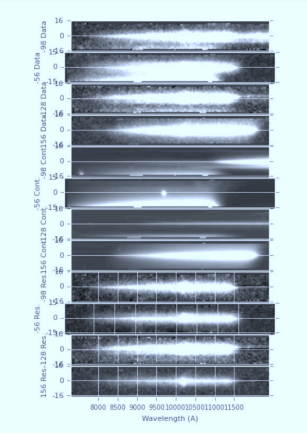
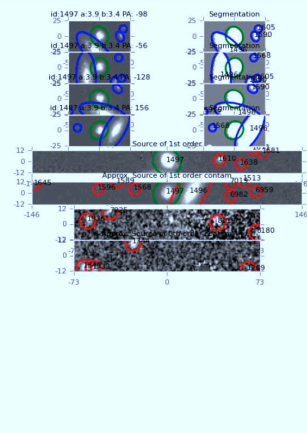


Radio sources in GOODS-N1: FIGS ID + images + 2D & 1D spectra

1497

189.156830
62.296238
(197.5)
(703.3)

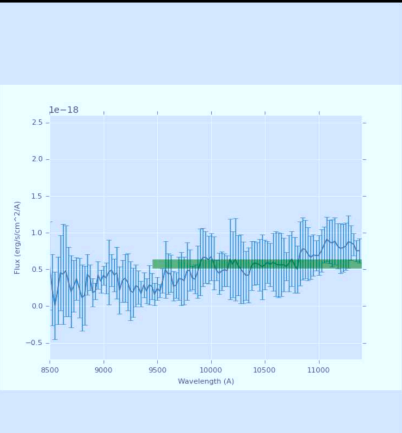
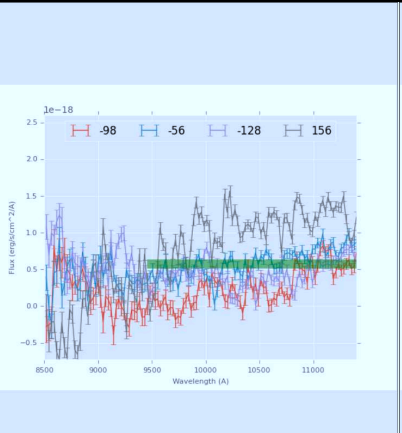
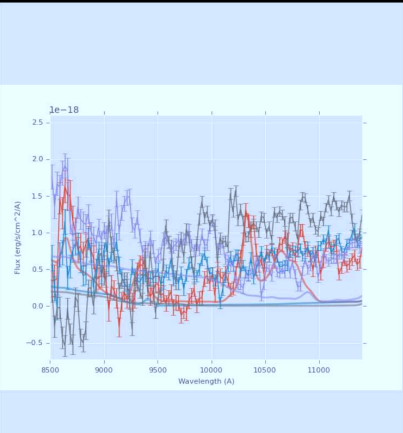
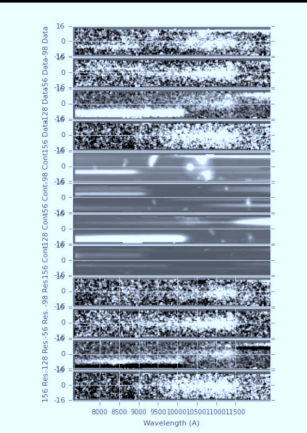
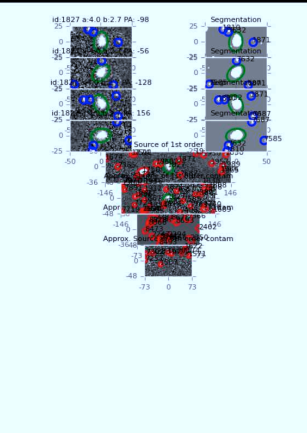
20.57



1827

189.175858
62.289585
(419.0)
(483.4)

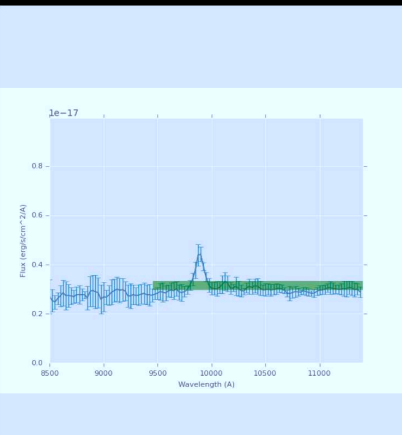
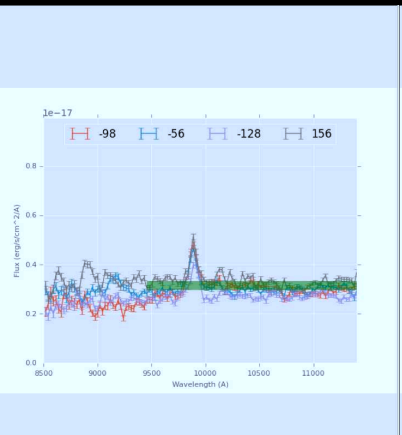
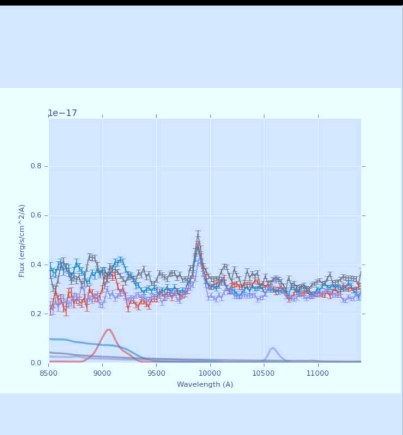
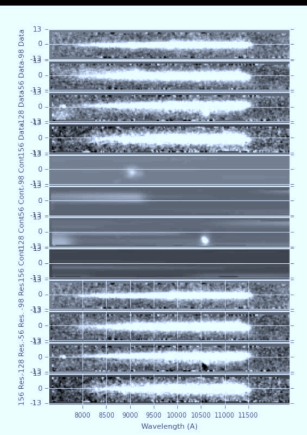
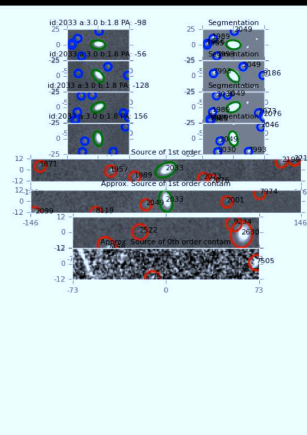
23.09



2033

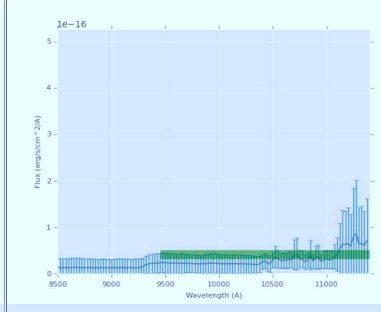
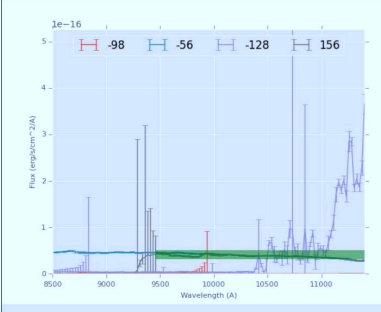
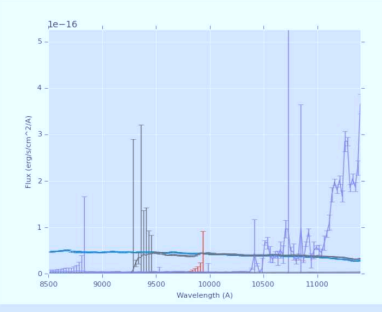
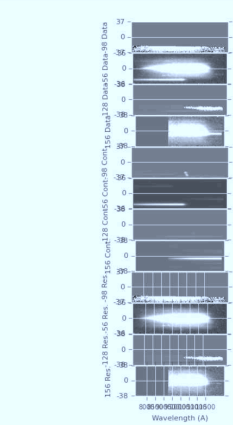
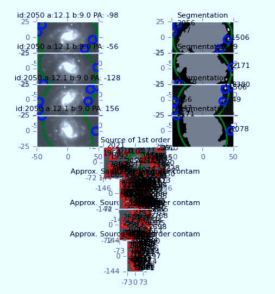
189.182953
62.284897
(562.8)
(413.3)

21.24

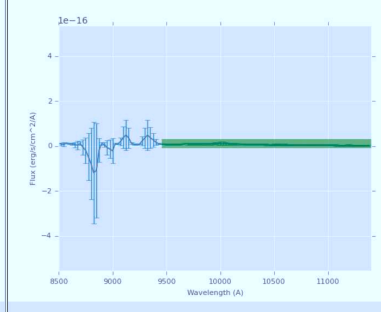
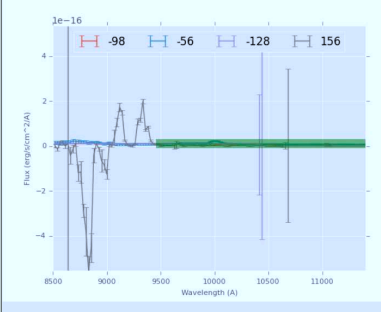
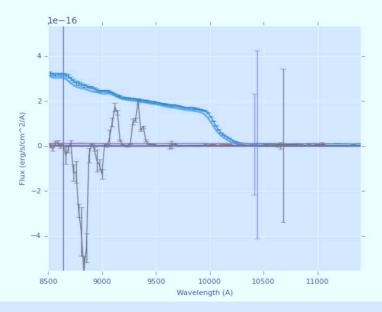
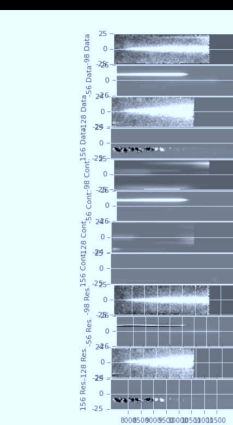
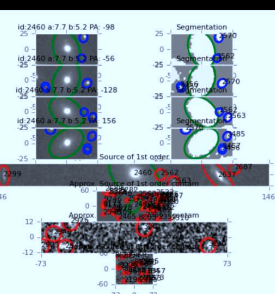


Radio sources in GOODS-N1: FIGS ID + images + 2D & 1D spectra

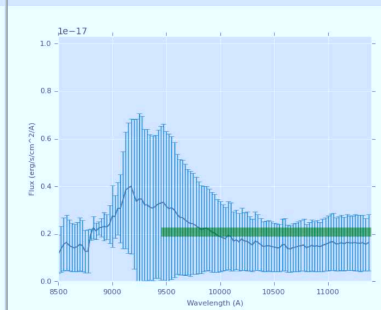
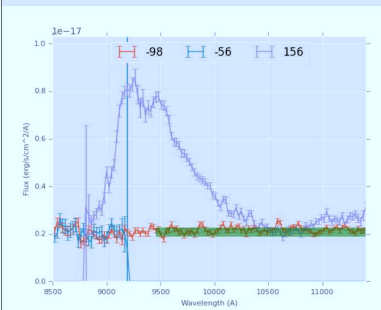
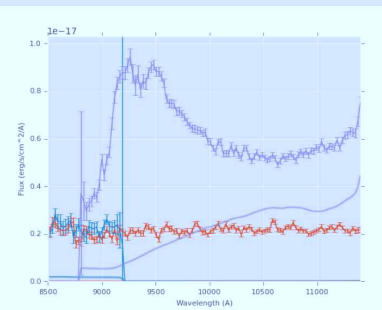
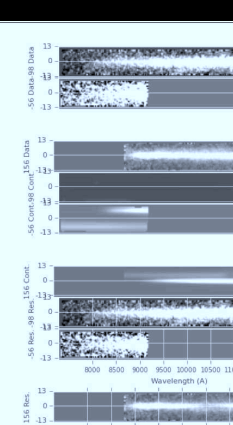
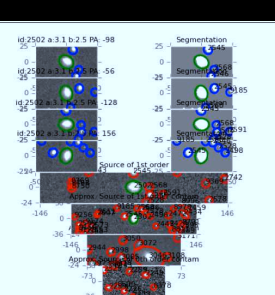
2050
 189.135483
 62.283173
 1011.9 1526.2
 (518.9)
 (1033.2)
 18.45



2460
 189.193085
 62.274826
 1355.0 817.2
 (862.0)
 (524.2)
 19.96



2502
 189.145264
 62.274536
 1270.6
 1436.1
 (777.6)
 (943.1)
 21.69

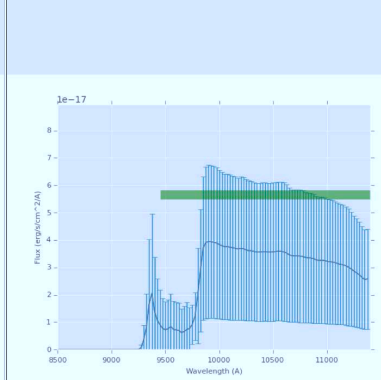
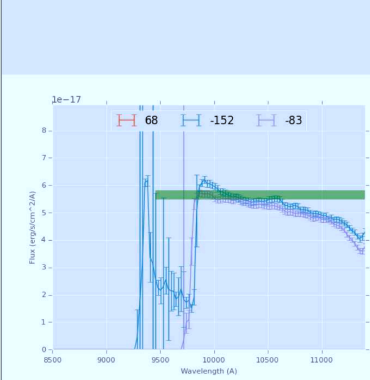
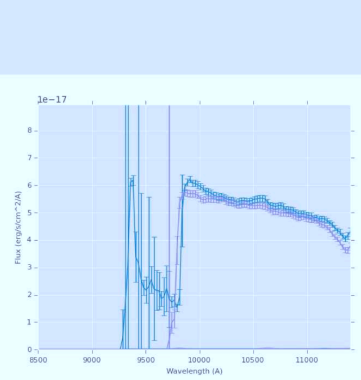
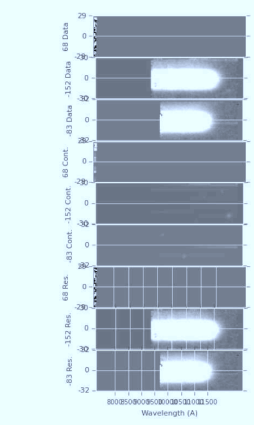
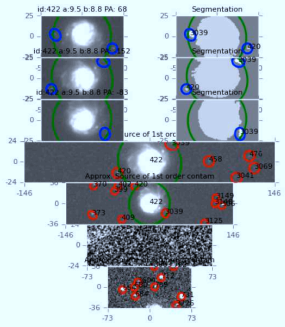


Radio sources in GOODS-N1: FIGS ID + images + 2D & 1D spectra

422

189.356384
62.328171
(1032.3)
(456.6)

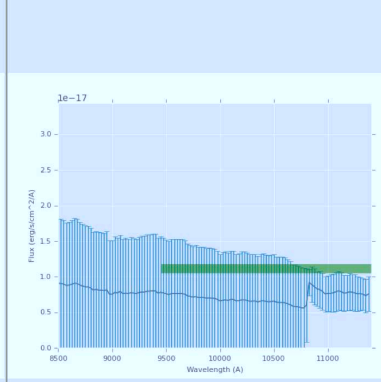
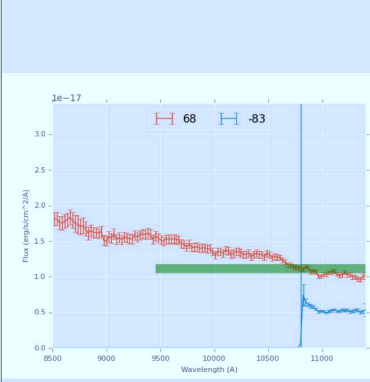
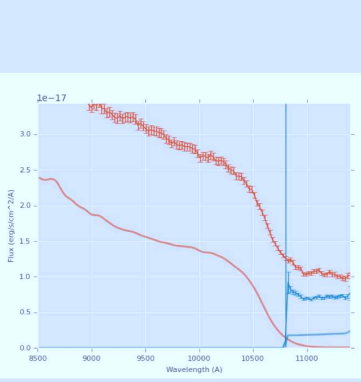
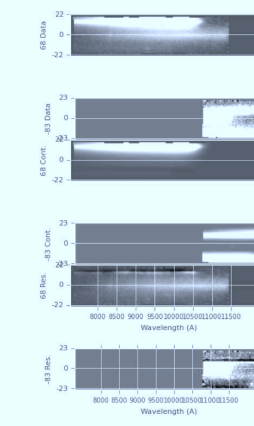
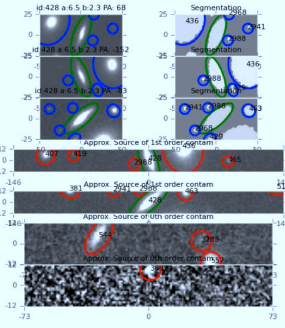
18.11



428

189.389618
62.328360
(1363.5)
(1351.5)
(870.5)
(858.5)

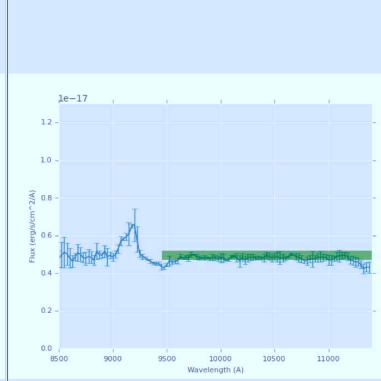
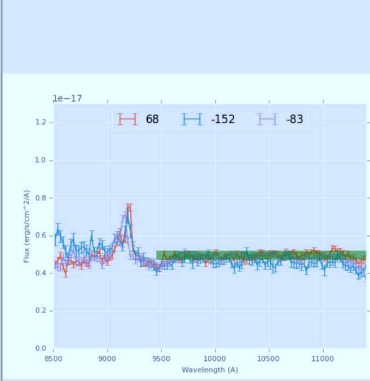
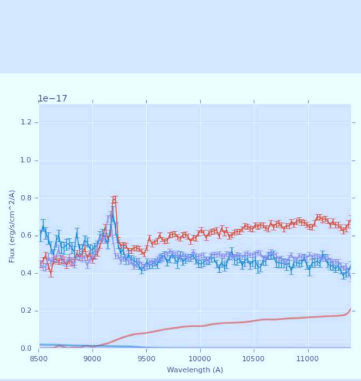
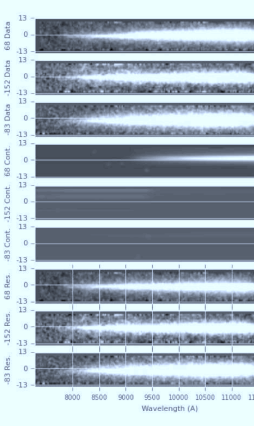
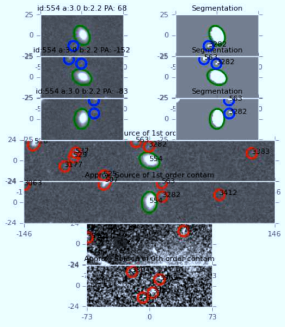
19.87



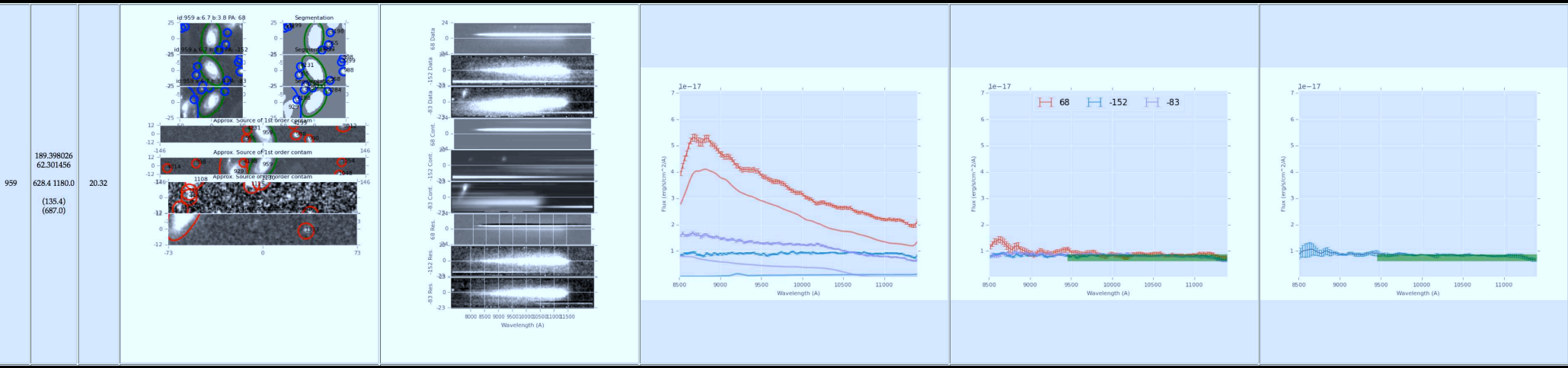
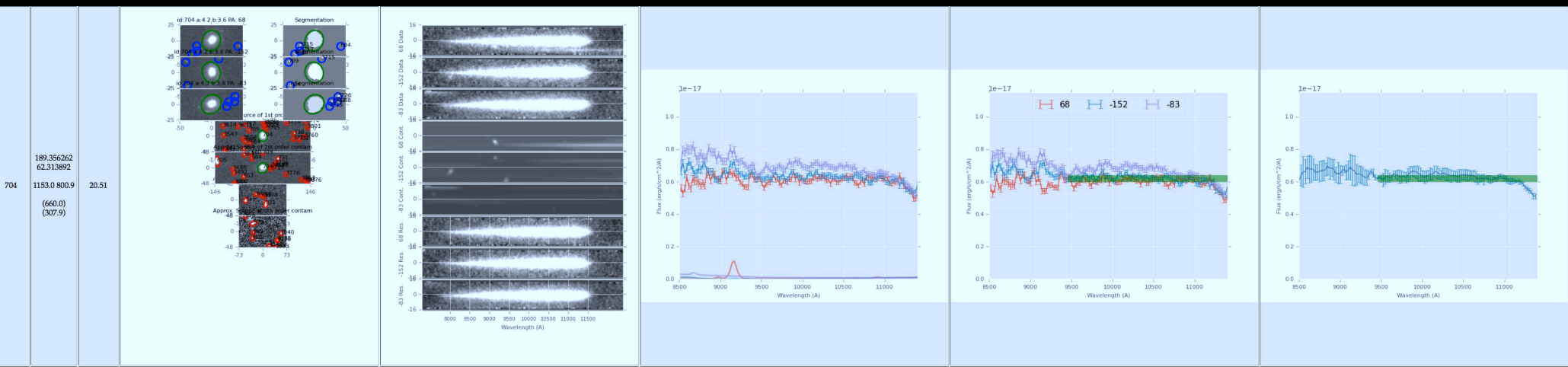
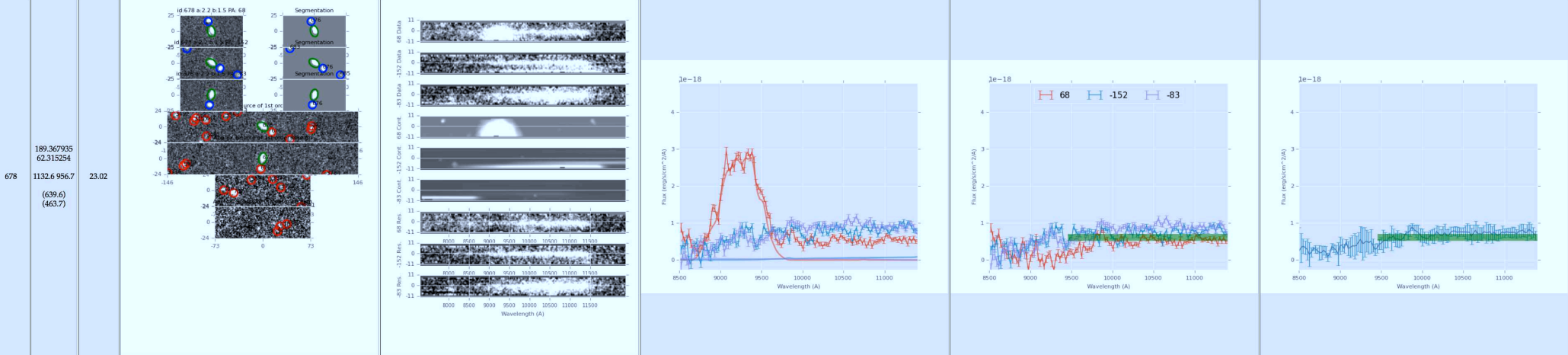
554

189.397171
62.321640
(1159.6)
(1377.1)
(666.6)
(884.1)

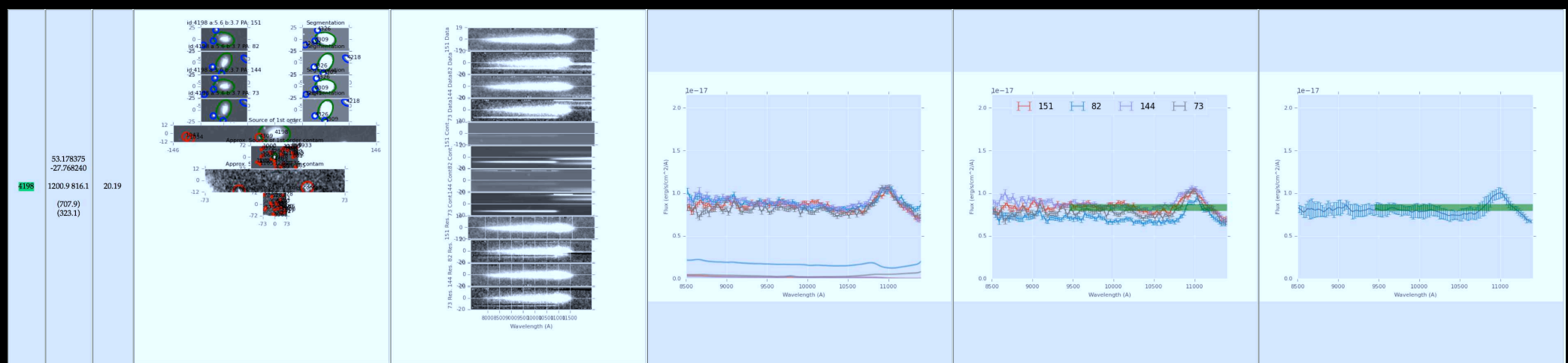
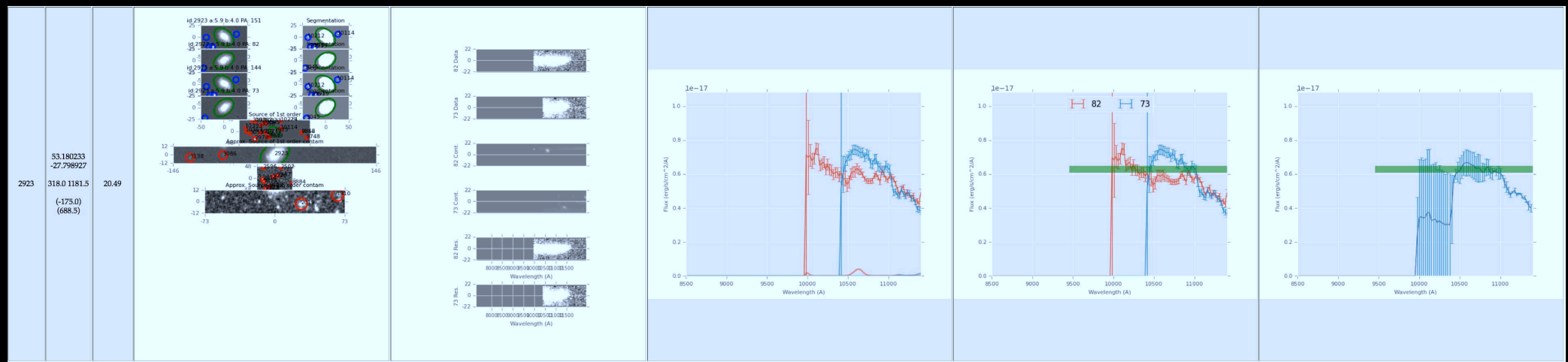
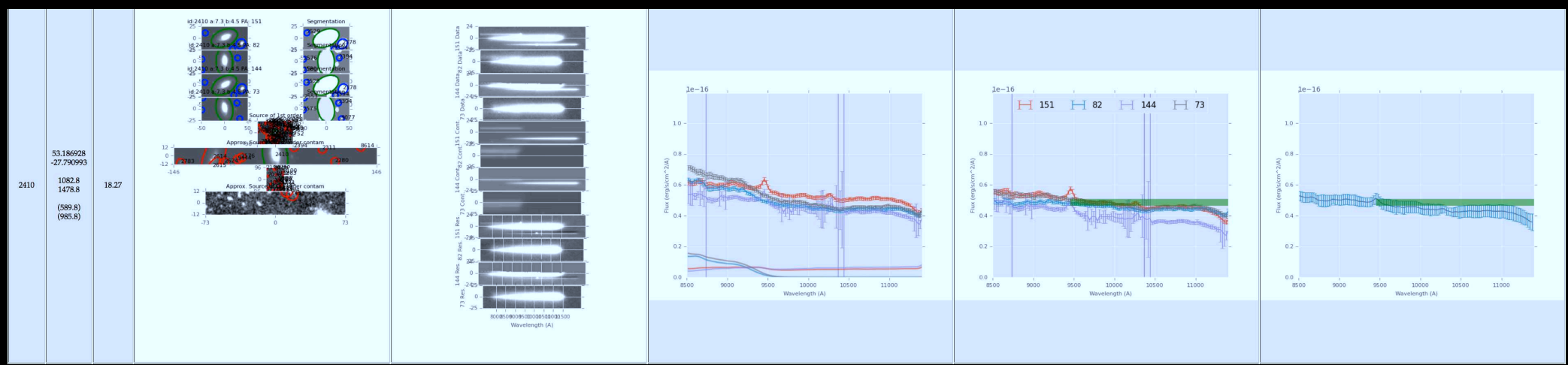
20.75



Radio sources in GOODS-N2: FIGS ID + images + 2D & 1D spectra



Radio sources in GOODS-N2: FIGS ID + images + 2D & 1D spectra

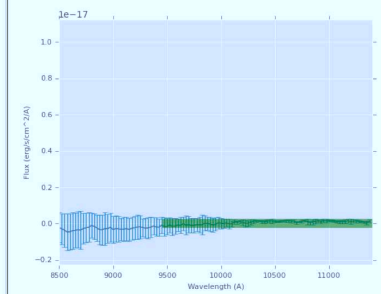
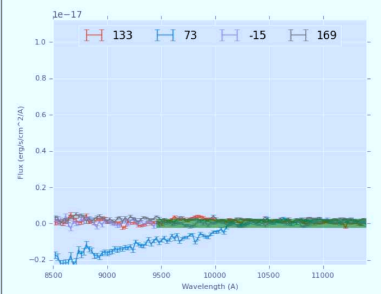
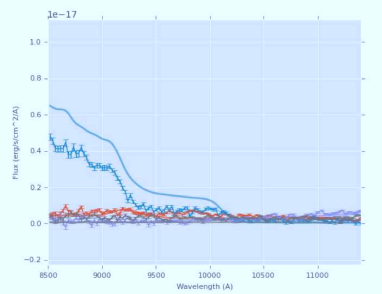
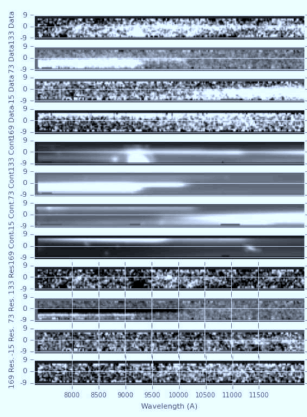
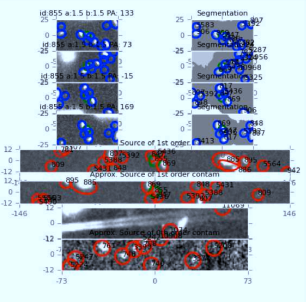


Radio sources in GOODS-S1: FIGS ID + images + 2D & 1D spectra

855

53.281116
-27.853547
(460.5
584.6)

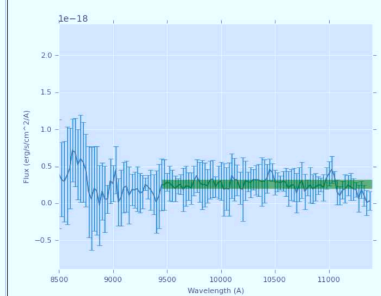
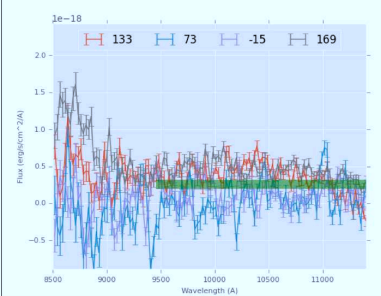
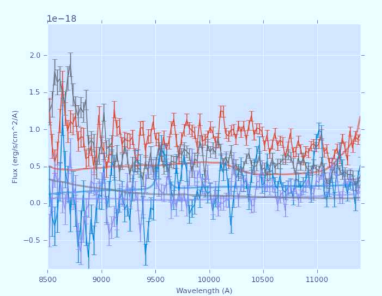
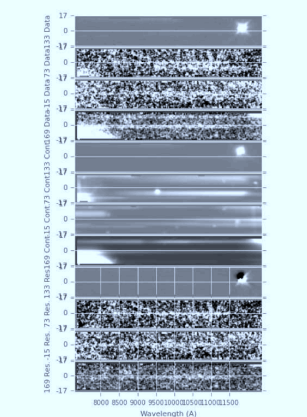
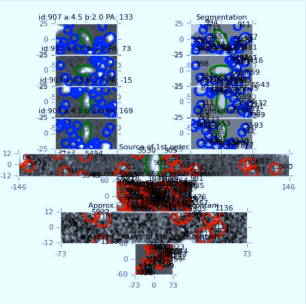
26.27



907

53.292213
-27.856960
(621.4
811.8)

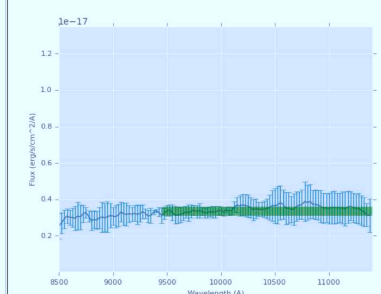
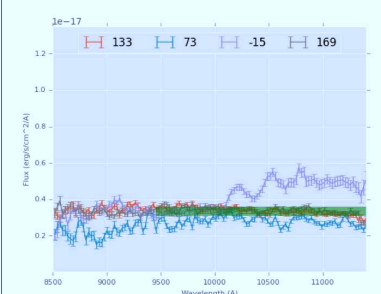
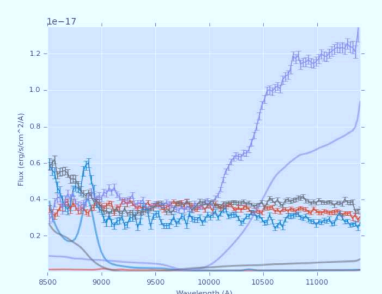
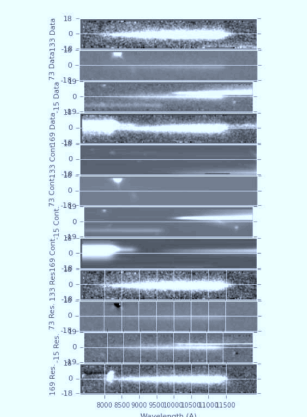
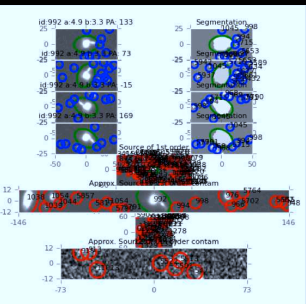
23.97



992

53.291241
-27.858679
(569.7
827.4)

21.18

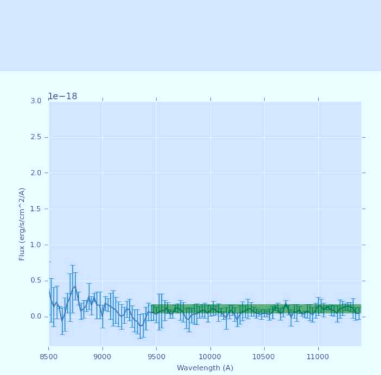
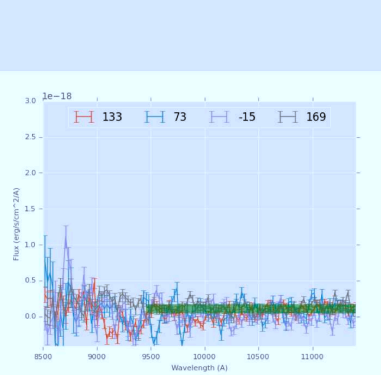
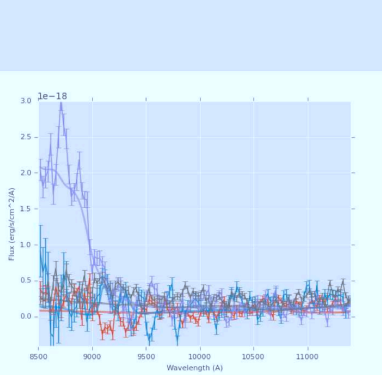
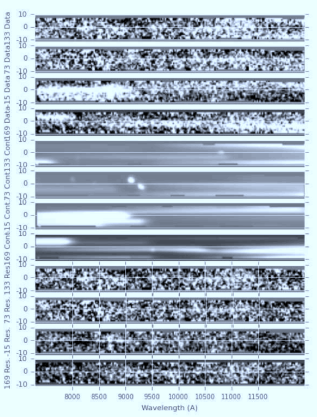
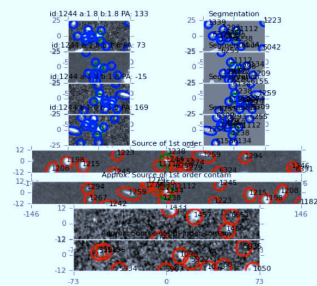


Radio sources in GOODS-S2: FIGS ID + images + 2D & 1D spectra

1244

53.262676
-27.862692
(0.0) (390.7)

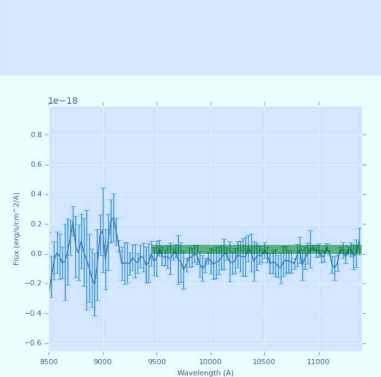
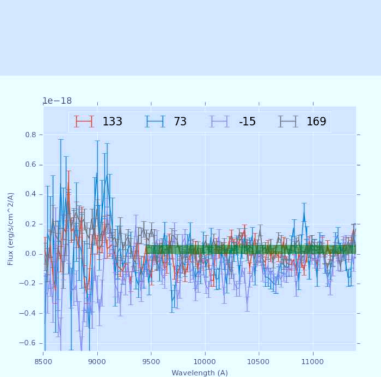
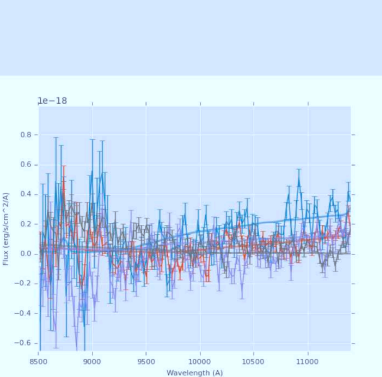
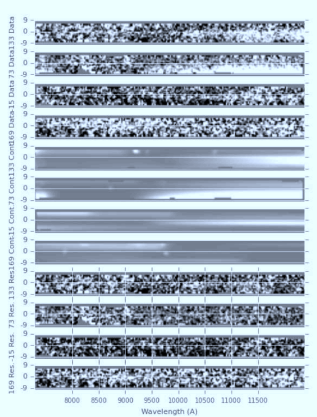
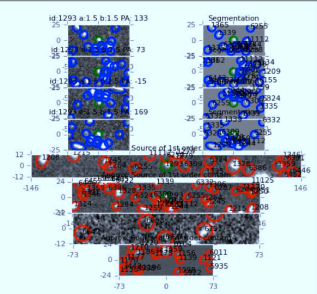
24.95



1293

53.262486
-27.863377
(-17.2)
(400.5)

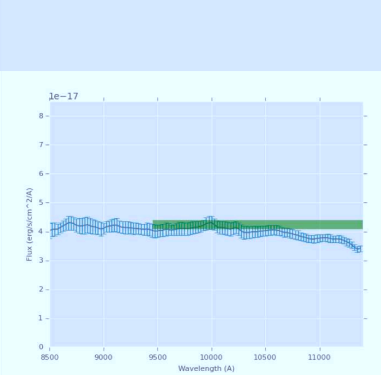
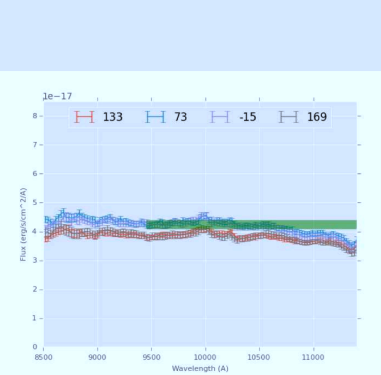
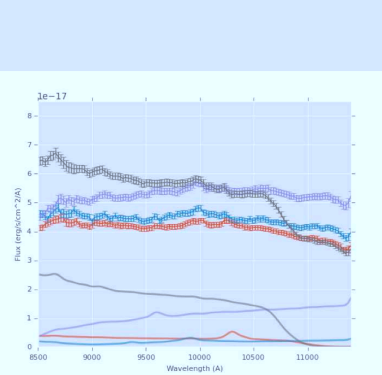
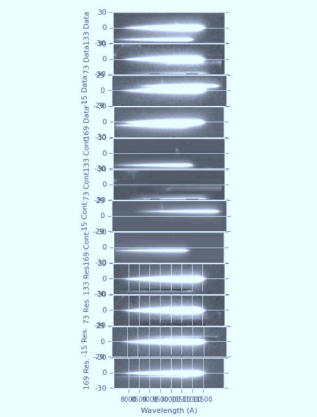
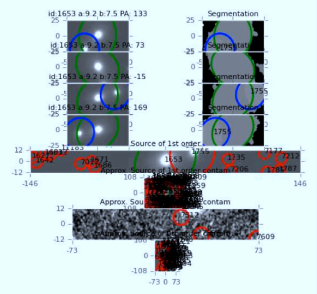
26.26



1653

53.273643
-27.870647
(25.4) (741.8)

18.42



Radio sources in GOODS-S2: FIGS ID + images + 2D & 1D spectra

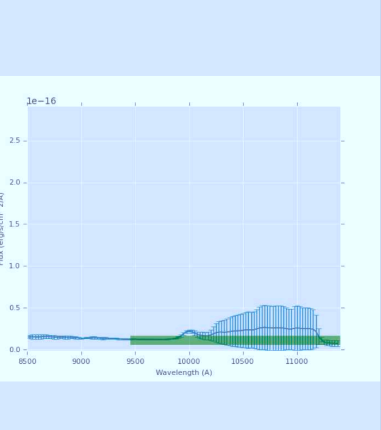
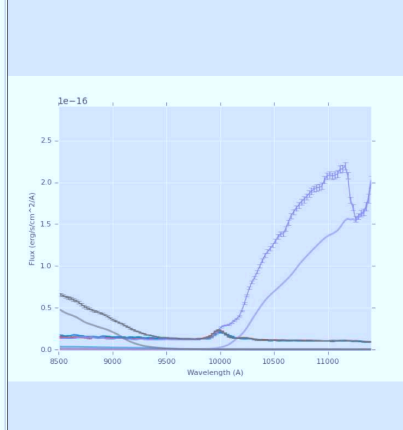
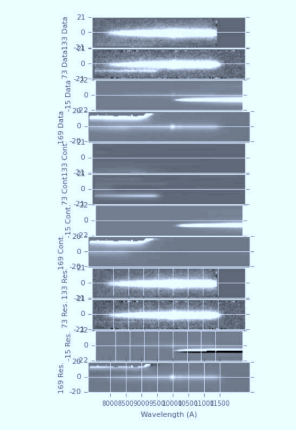
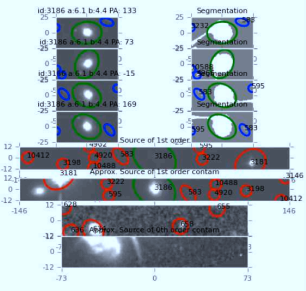
3186

53.291828
-27.845343

1344.3
1073.3

(851.3)
(580.3)

19.89

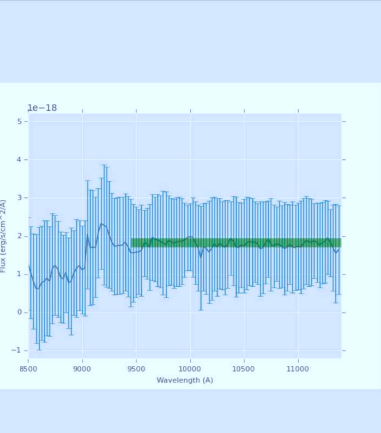
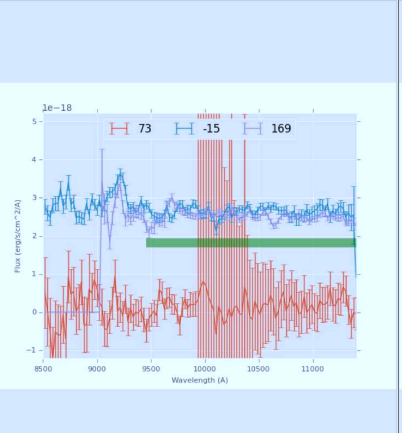
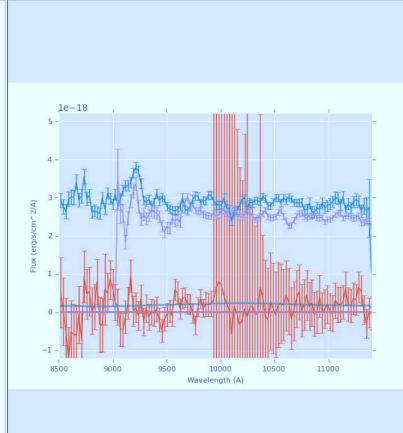
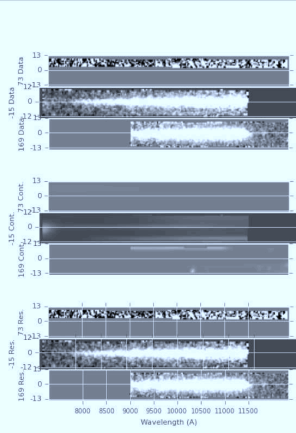
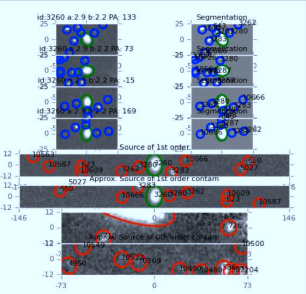


3260

53.254066
-27.848232

1244.3 525.2
(751.3) (32.2)

21.84

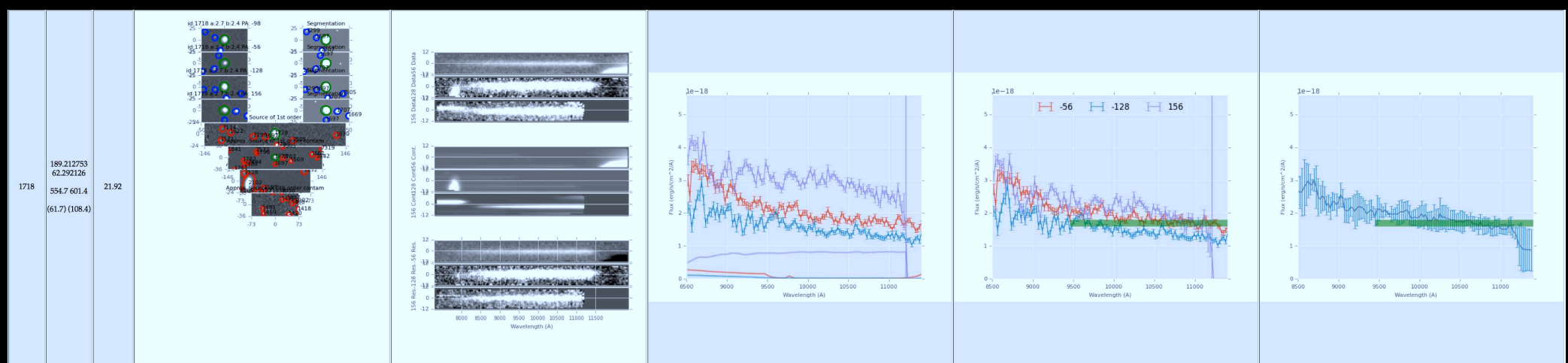
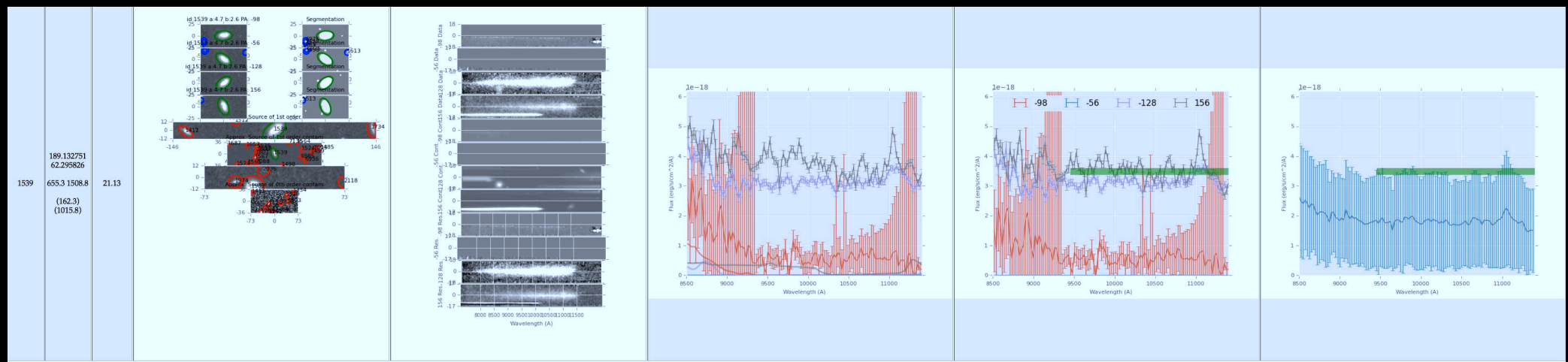
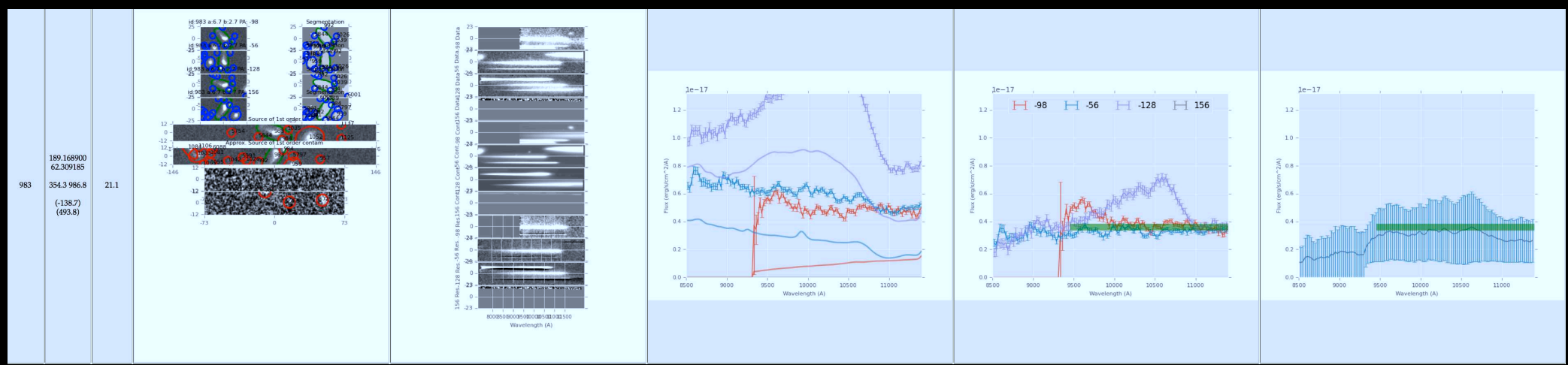


Radio sources in GOODS-S2: FIGS ID + images + 2D & 1D spectra

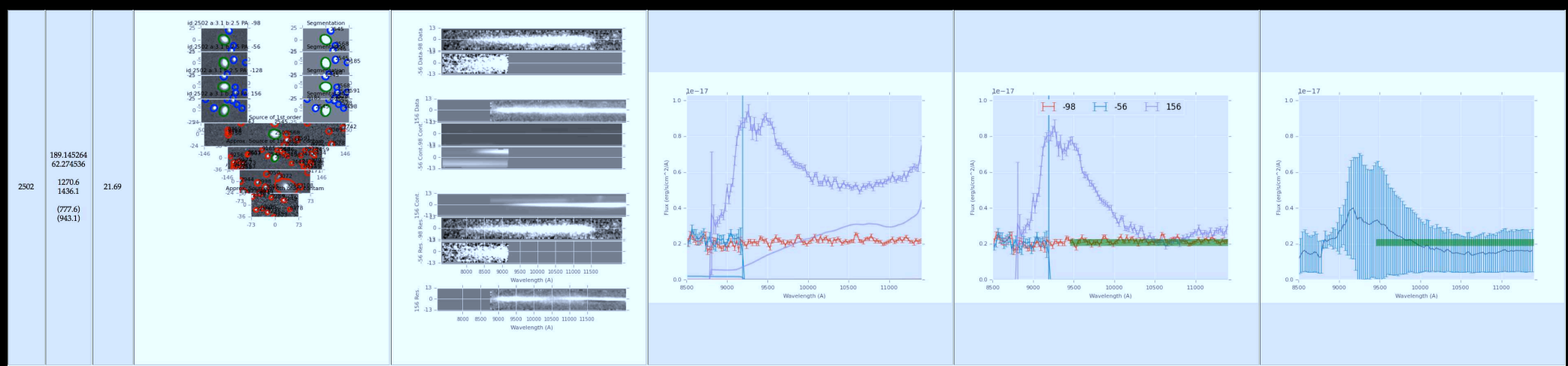
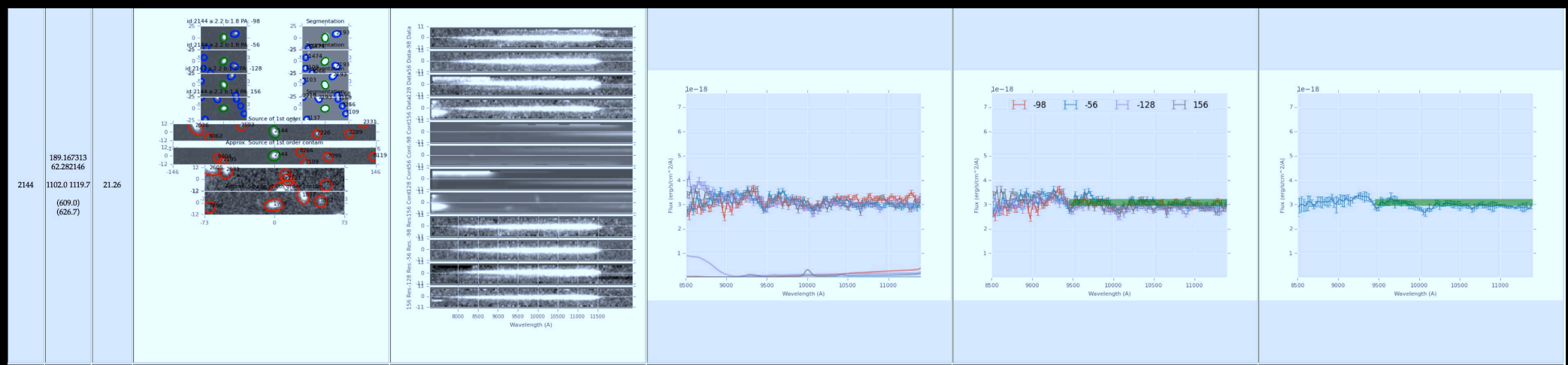
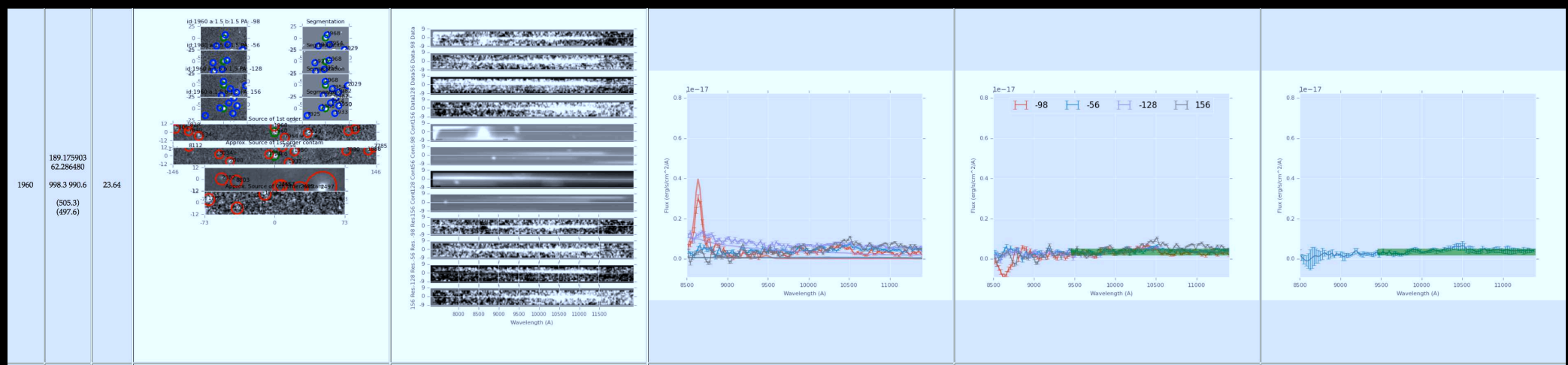
X-ray Sources with FIGS spectra

Reference	Fld	Instr. keV	5σ (cgs)	FWHM ($''$)	N_{FIGS}/N_{XRSS}
Alexander ⁺ 2003 AJ, 126, 539	G-N	CXO 0.5–2	2.5E-17	2 $''$	9/39+8/21 =17/60
Xue ⁺ 2011 ApJS, 195, 10	G-S	CXO 0.5–2	9.1E-18	2 $''$	30/108+6/17=36/125
TOTAL					53/185 (29%)

- Position error $\simeq 0.42 * \text{FWHM} / (\text{S/N-ratio})$.
 - FIGS spectra available for X-ray sources in $\sim 30\%$ of catalog search area.
- Following pages show all FIGS spectra in numerical order without filtering:



X-ray sources in GOODS-N1: FIGS ID + images + 2D & 1D spectra

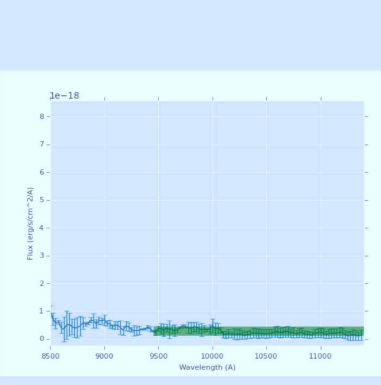
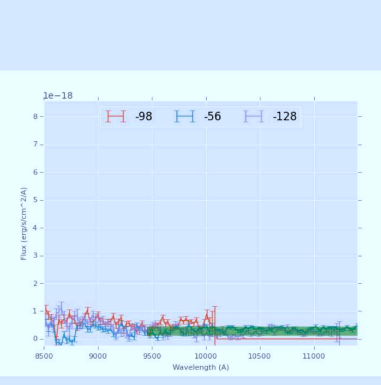
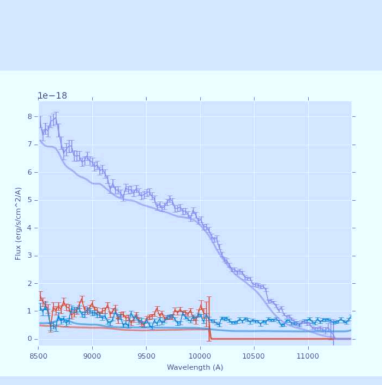
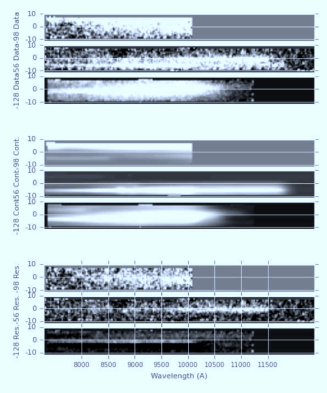
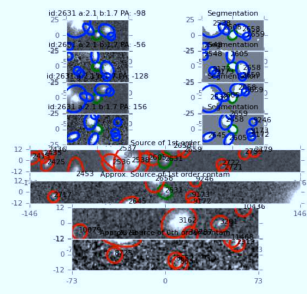


X-ray sources in GOODS-N1: FIGS ID + images + 2D & 1D spectra

2631

189.182968
62.272472
1400.8 957.6
(907.8)
(464.6)

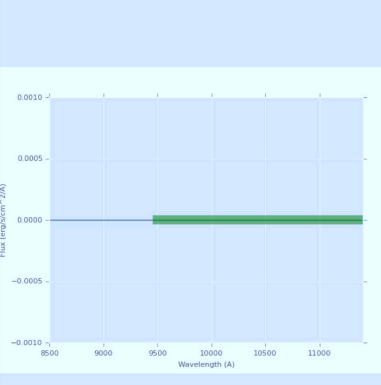
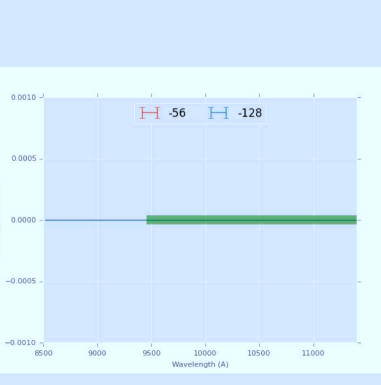
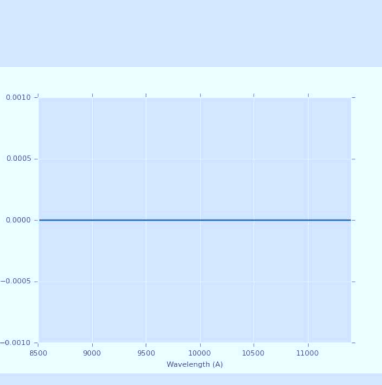
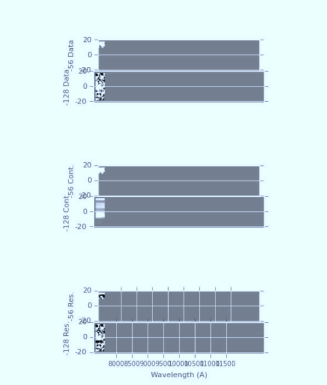
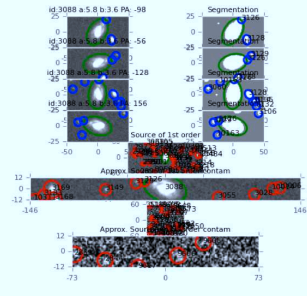
23.83



3088

189.175797
62.262627
1511.5 546.4
(1018.5)
(53.4)

20.54

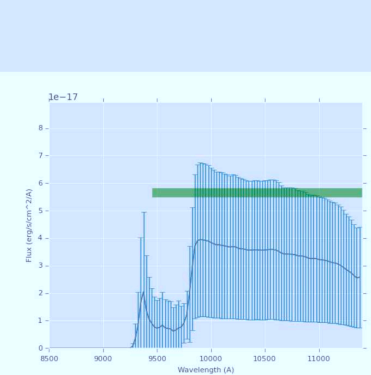
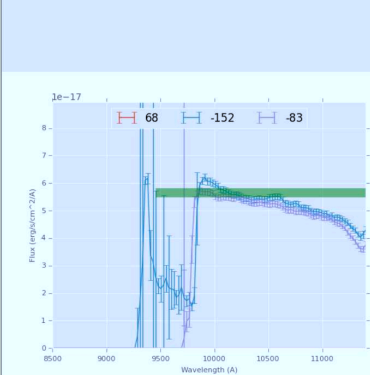
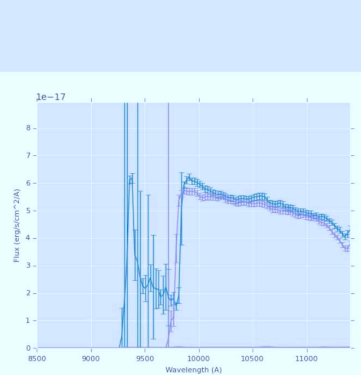
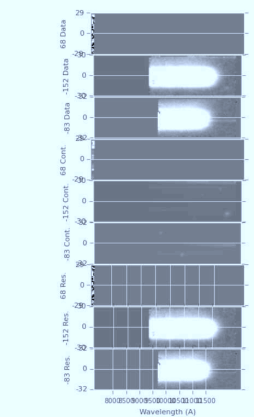
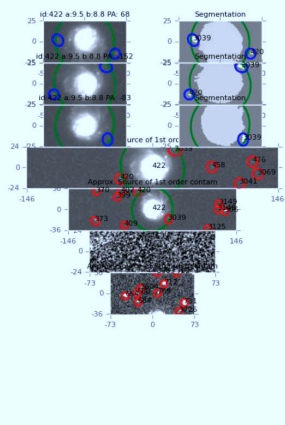


X-ray sources in GOODS-N1: FIGS ID + images + 2D & 1D spectra

422

189.356384
62.328171
1525.3 949.6
(103.3)
(456.6)

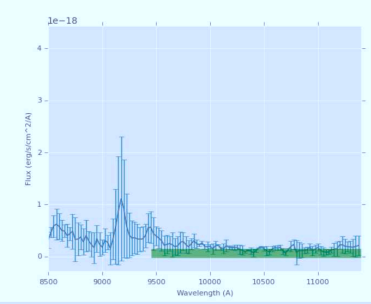
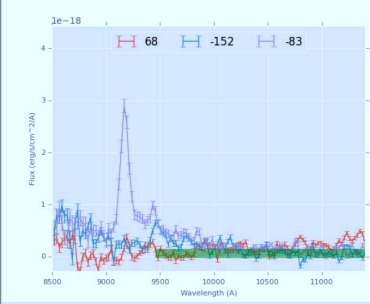
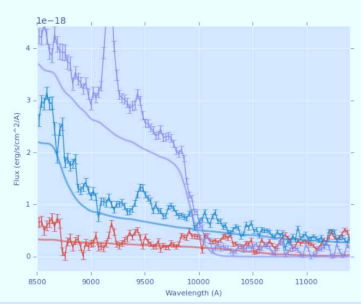
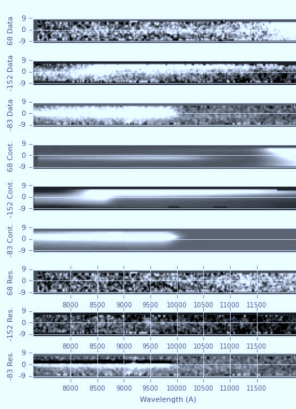
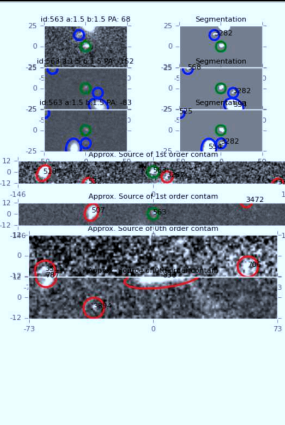
18.11



563

189.395340
62.321213
1157.2
1350.5
(664.2)
(857.5)

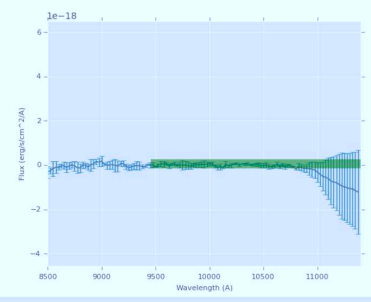
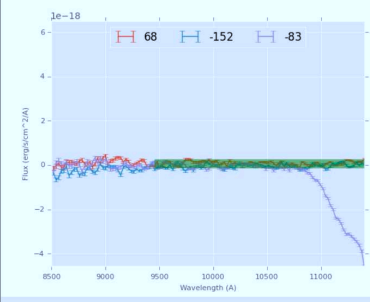
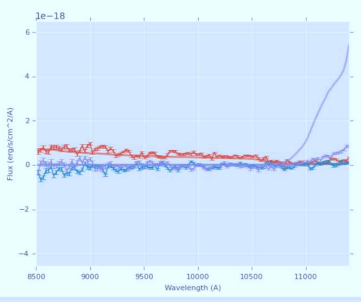
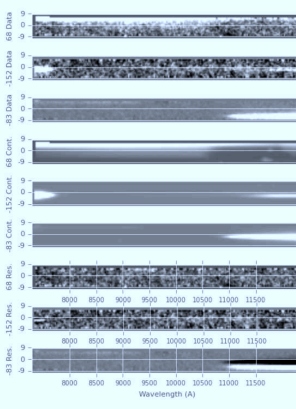
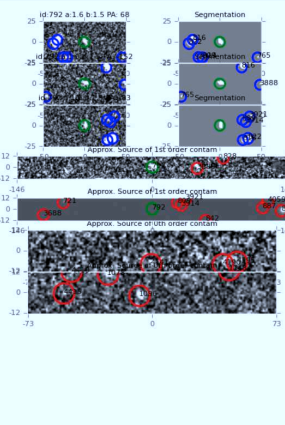
25.45



792

189.404404
62.309505
808.1 1340.2
(315.1)
(847.2)

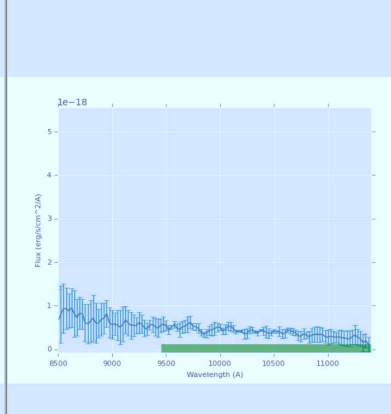
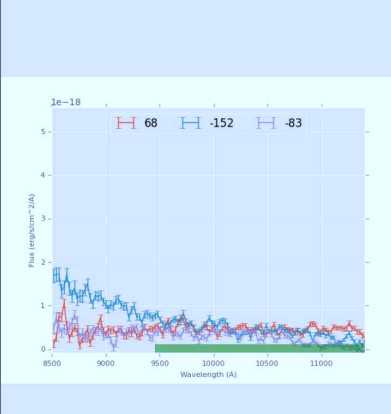
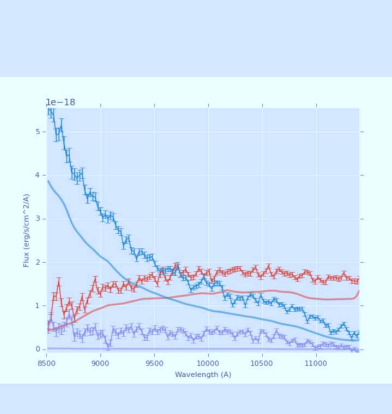
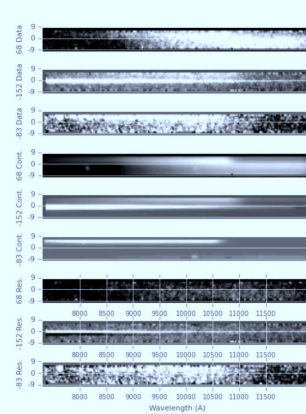
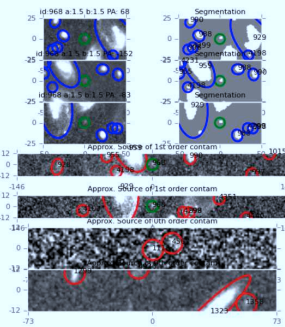
25.52



X-ray sources in GOODS-N2: FIGS ID + images + 2D & 1D spectra

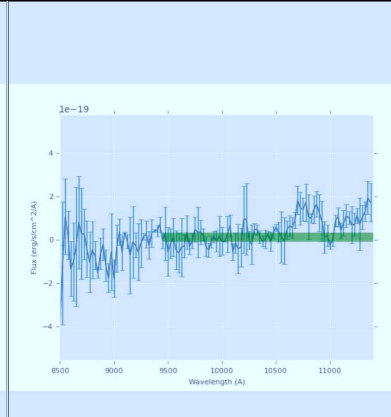
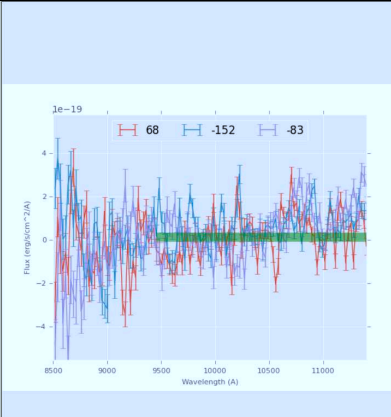
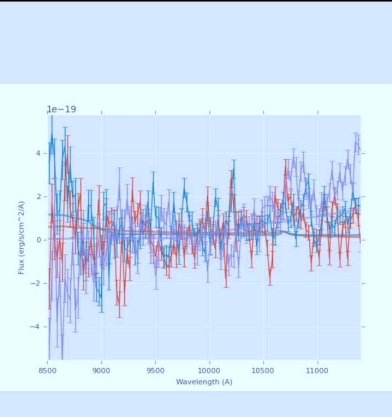
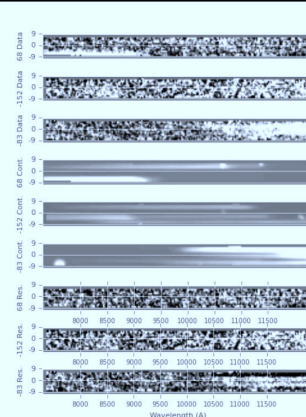
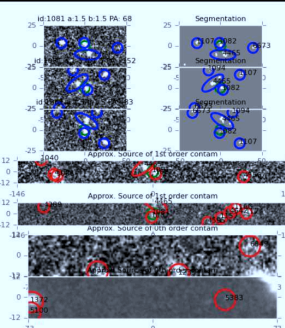
968
189.400330
62.301552
(126.8)
(715.9)

27.09



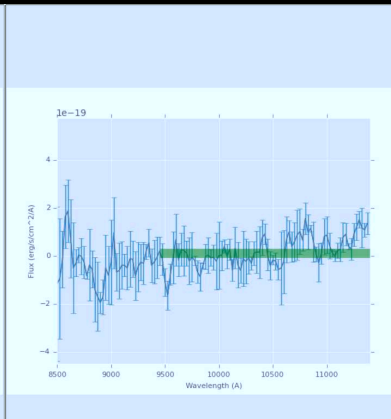
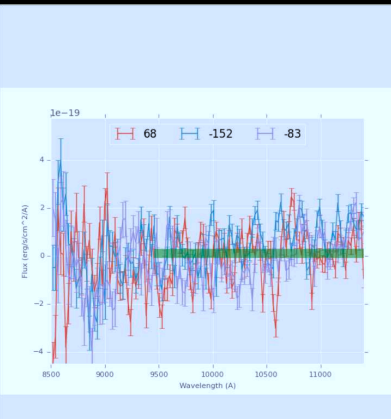
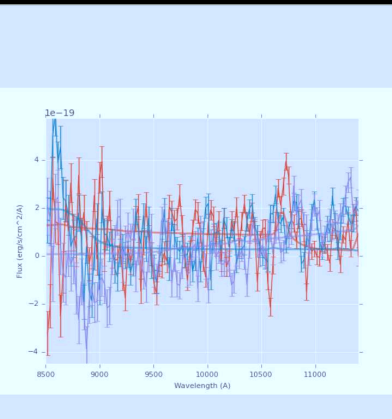
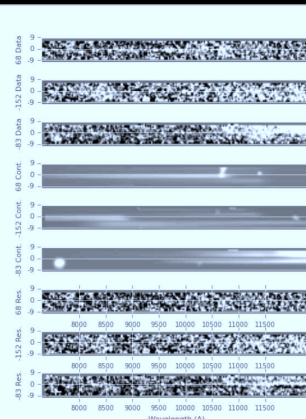
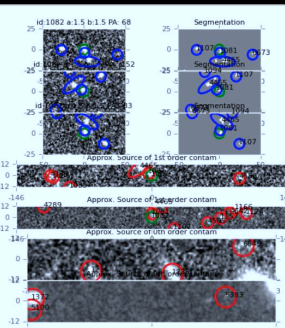
1081
189.361526
62.296524
(181.1)
(193.0)

27.1



1082
189.361832
62.296543
(180.2)
(196.9)

27.37

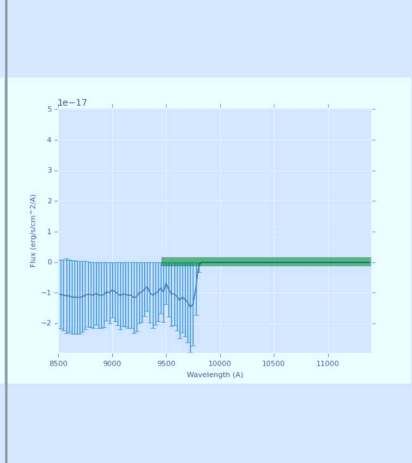
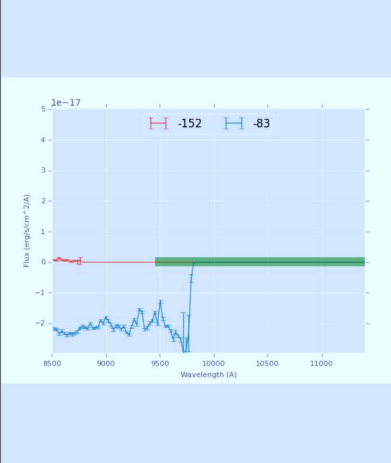
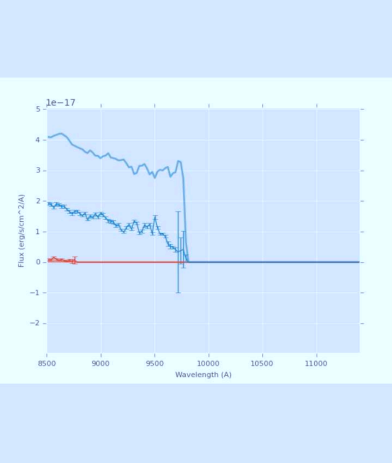
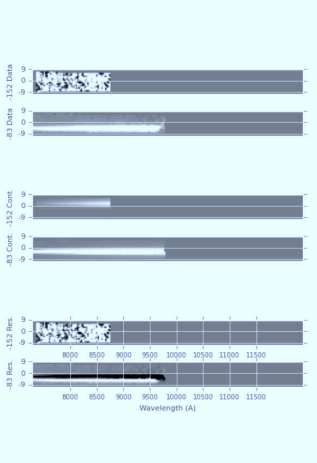
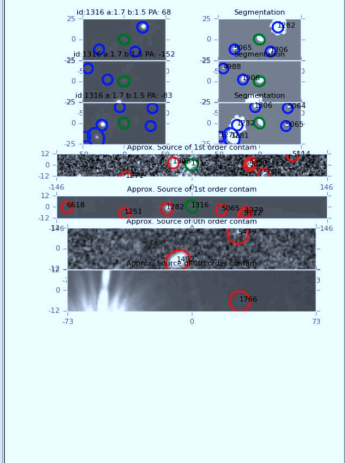


X-ray sources in GOODS-N2: FIGS ID + images + 2D & 1D spectra

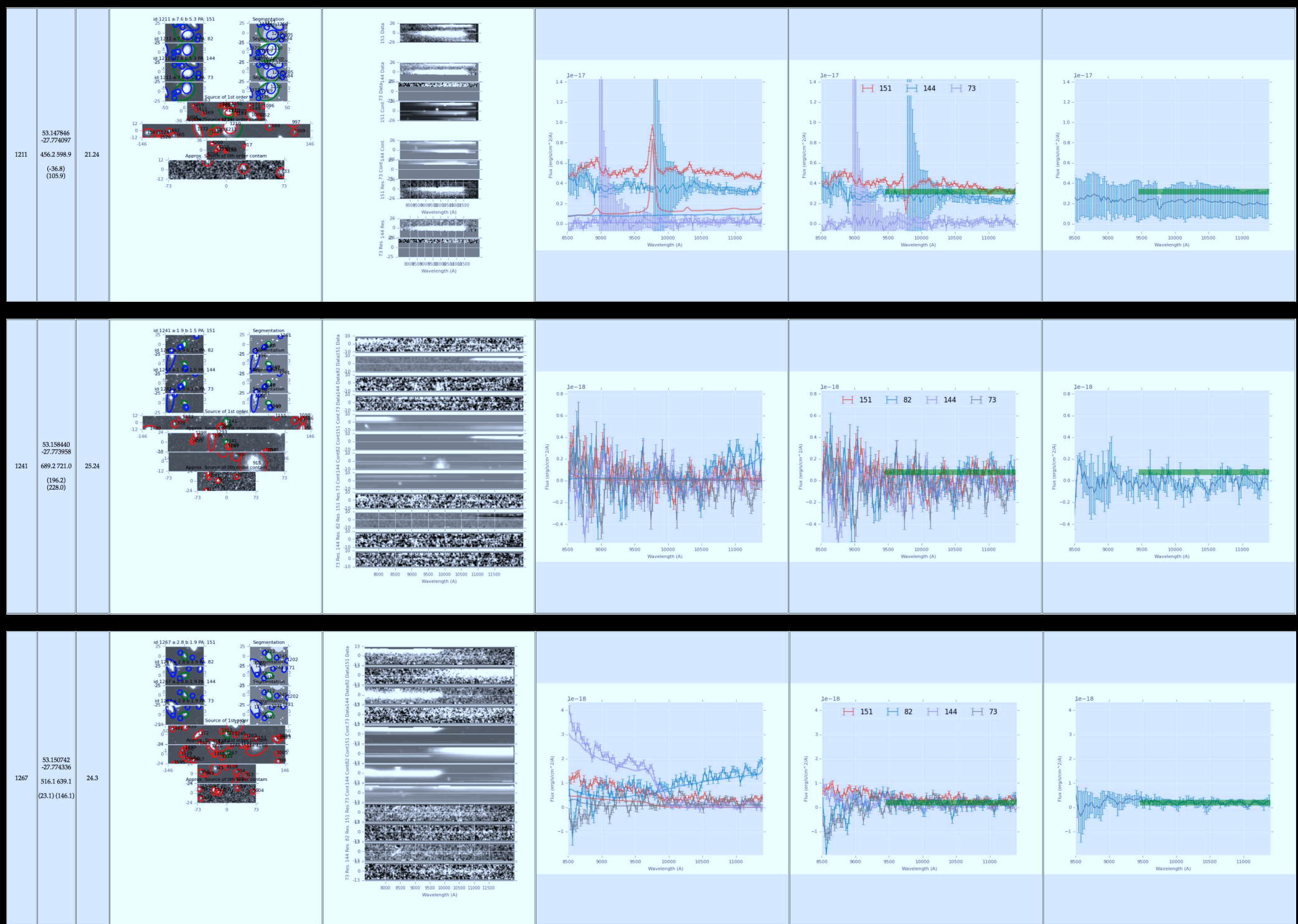
1316

189.408127
62.287109
1477.3
1343.6
(984.3)
(850.6)

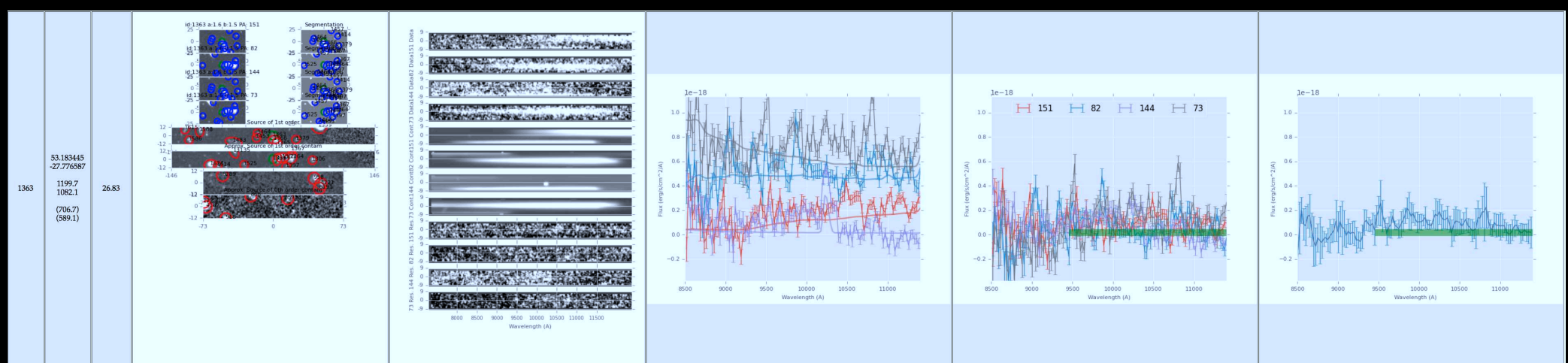
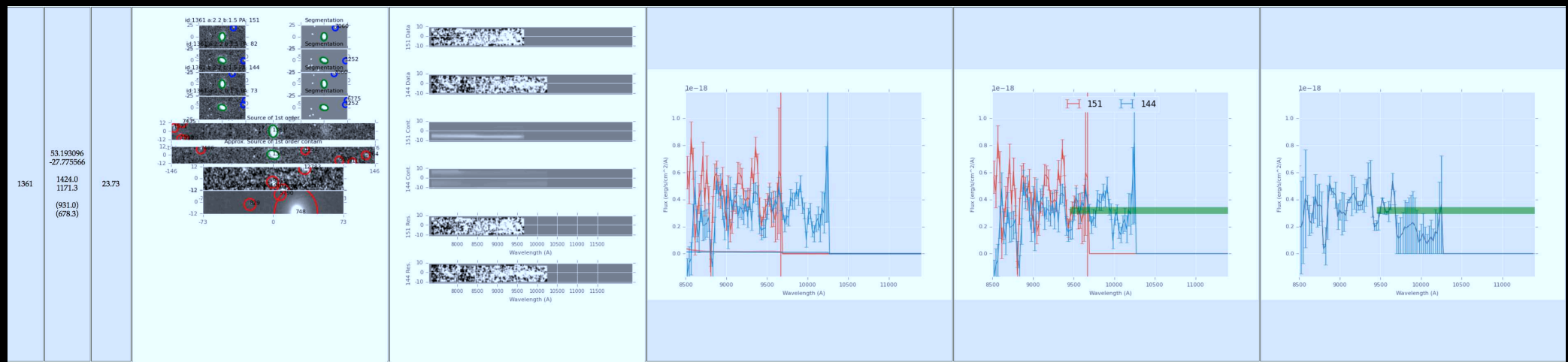
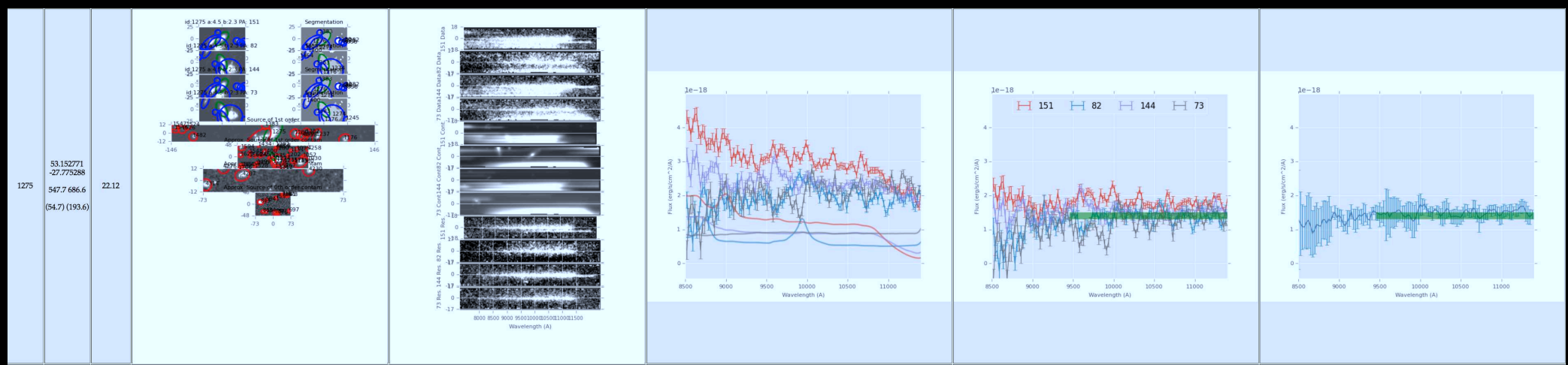
24.33



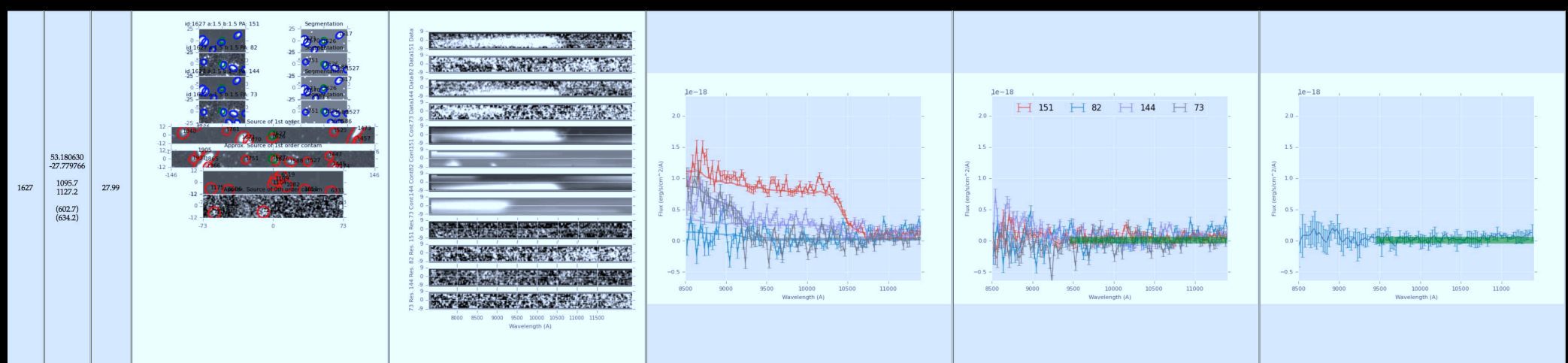
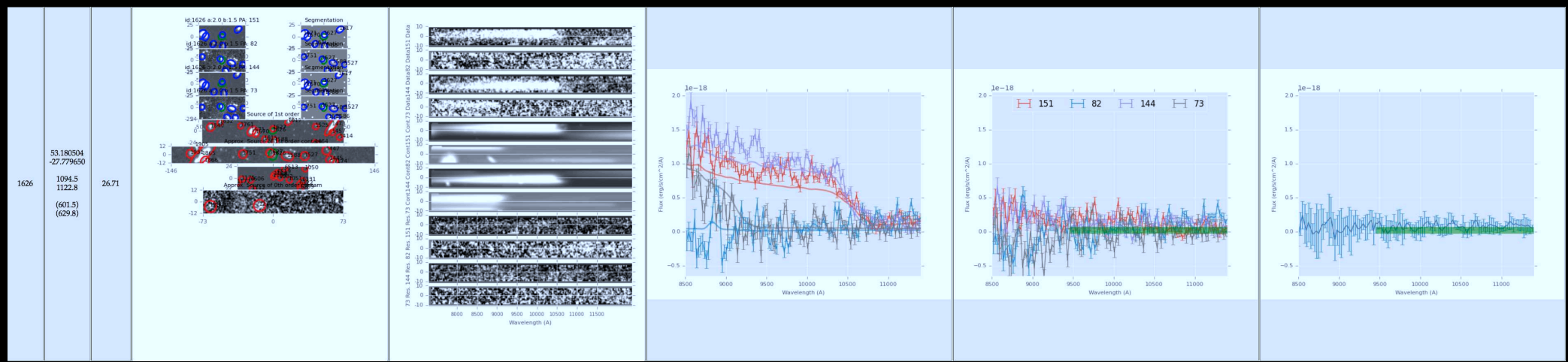
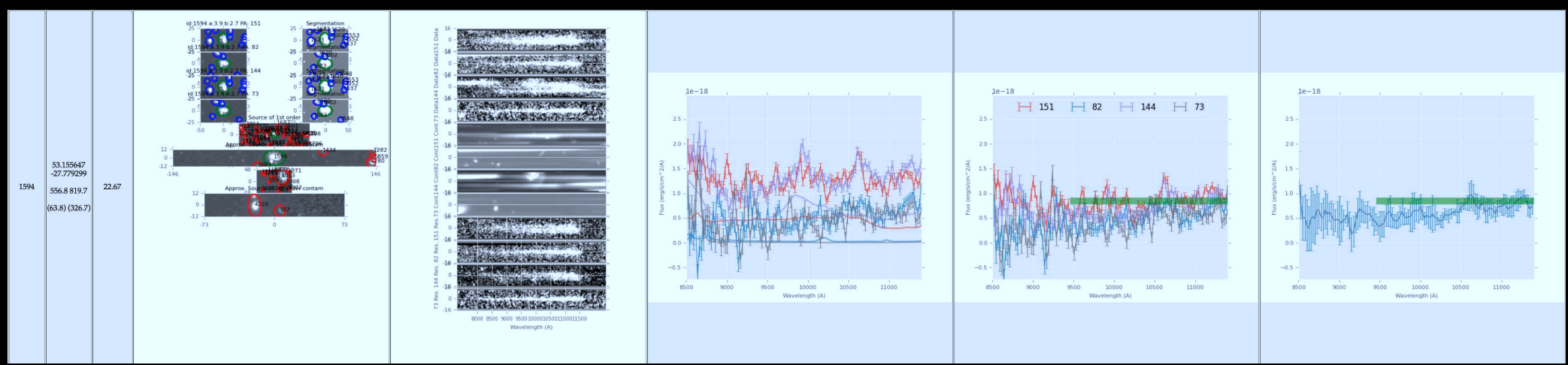
X-ray sources in GOODS-N2: FIGS ID + images + 2D & 1D spectra



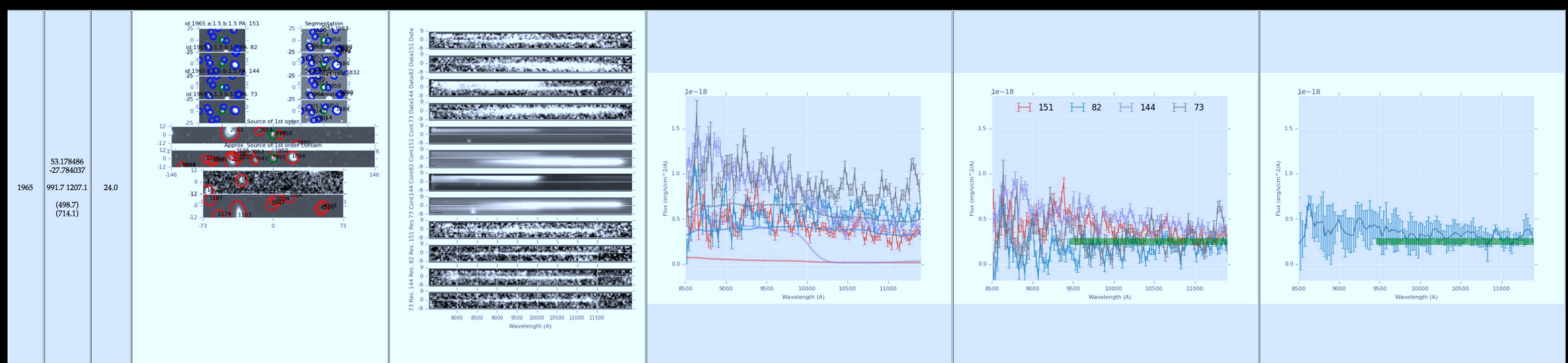
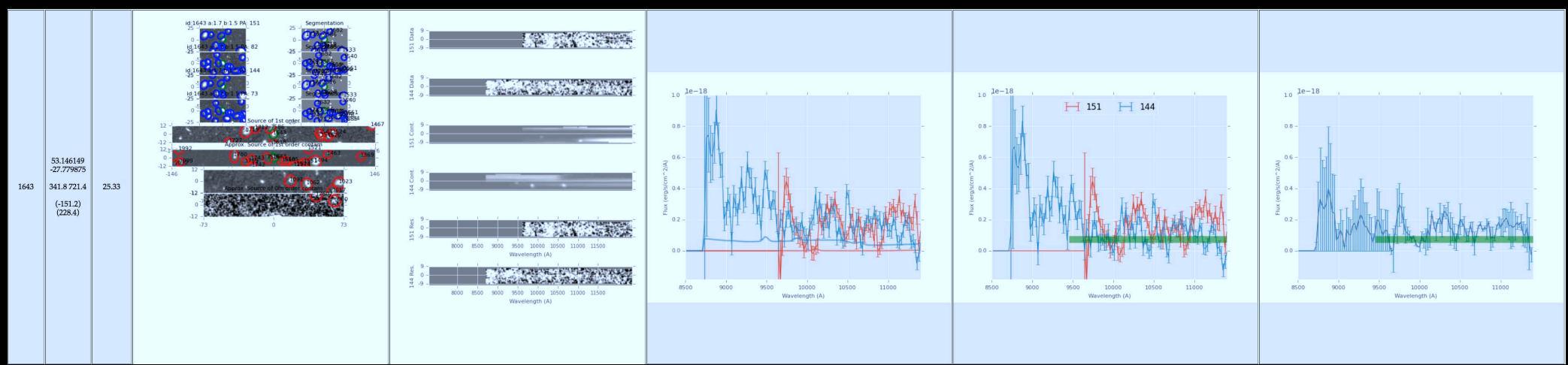
X-ray sources in GOODS-S1: FIGS ID + images + 2D & 1D spectra



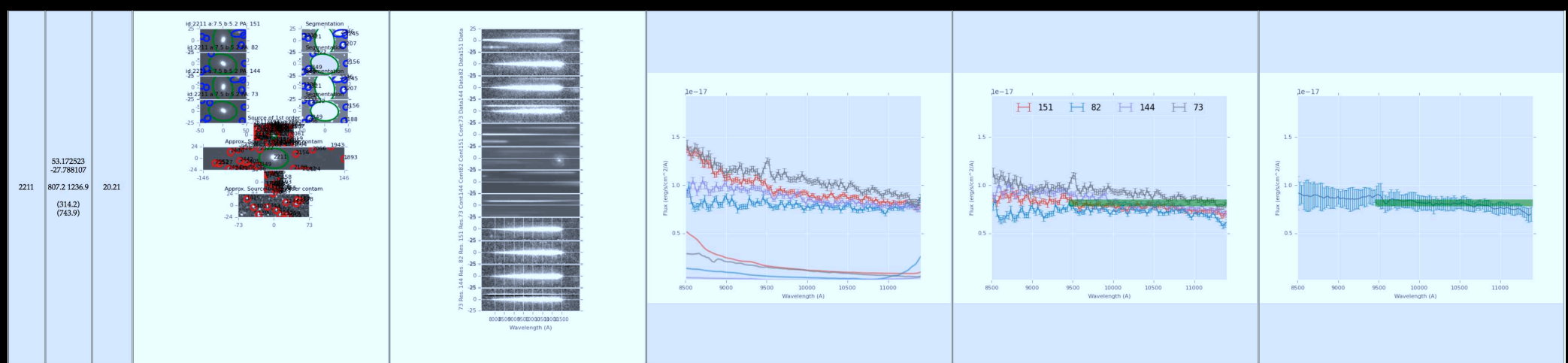
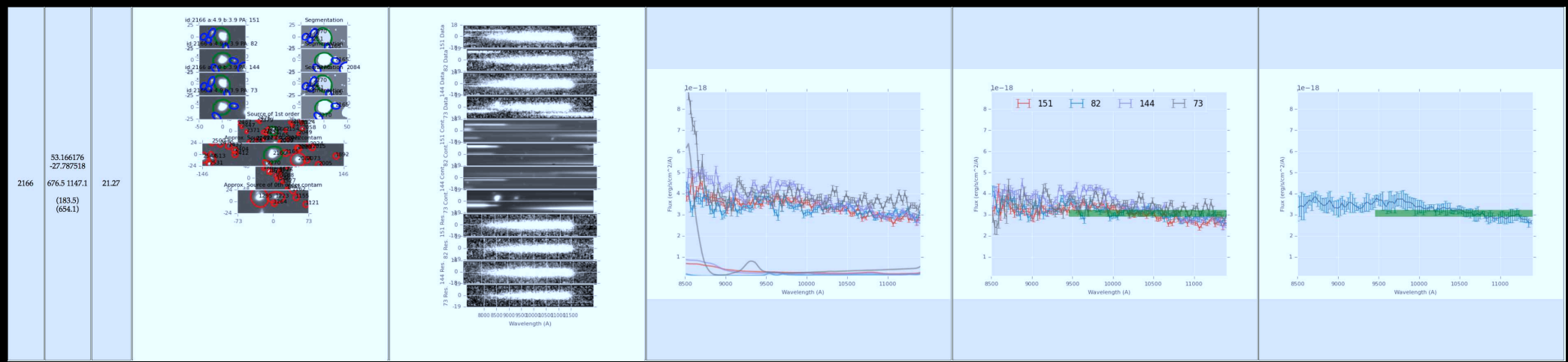
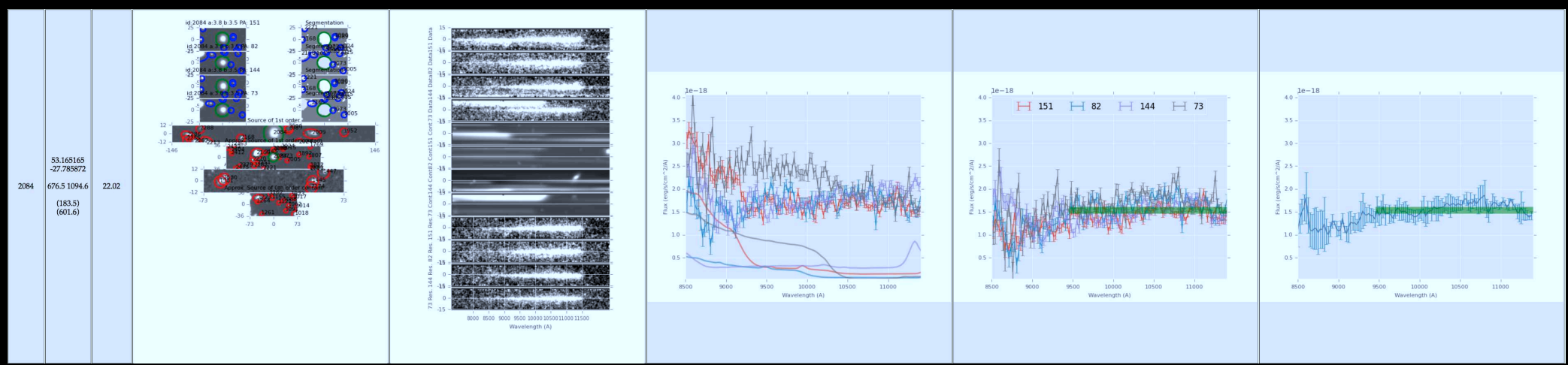
X-ray sources in GOODS-S1: FIGS ID + images + 2D & 1D spectra



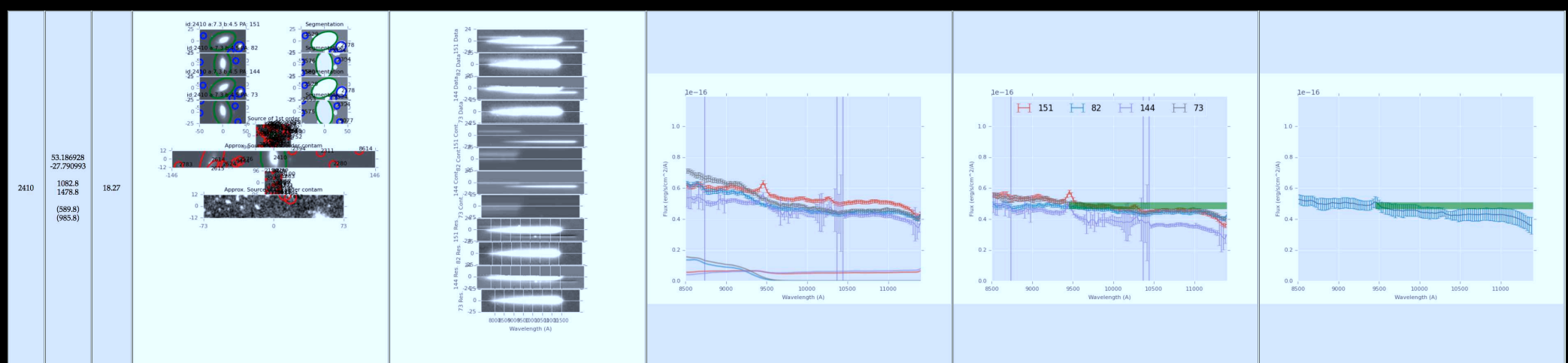
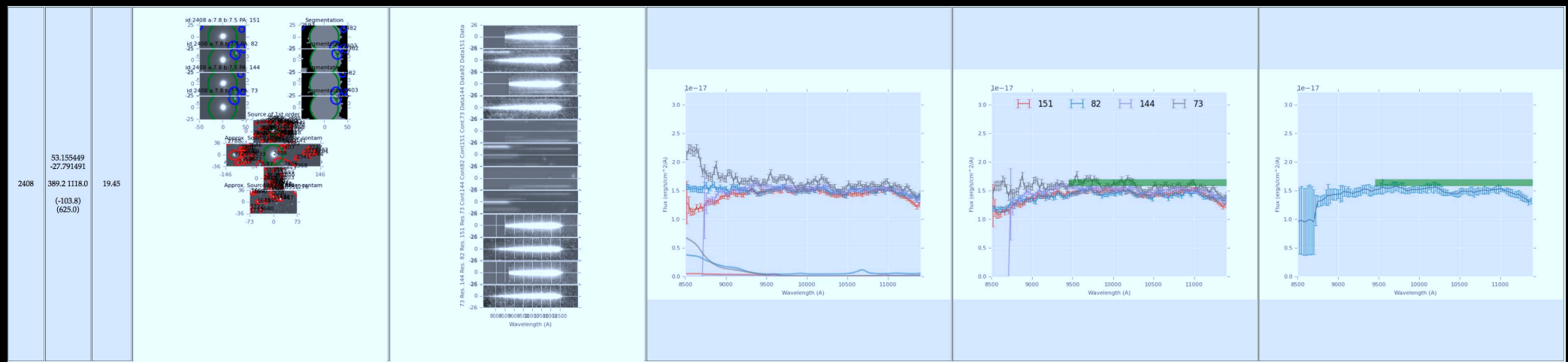
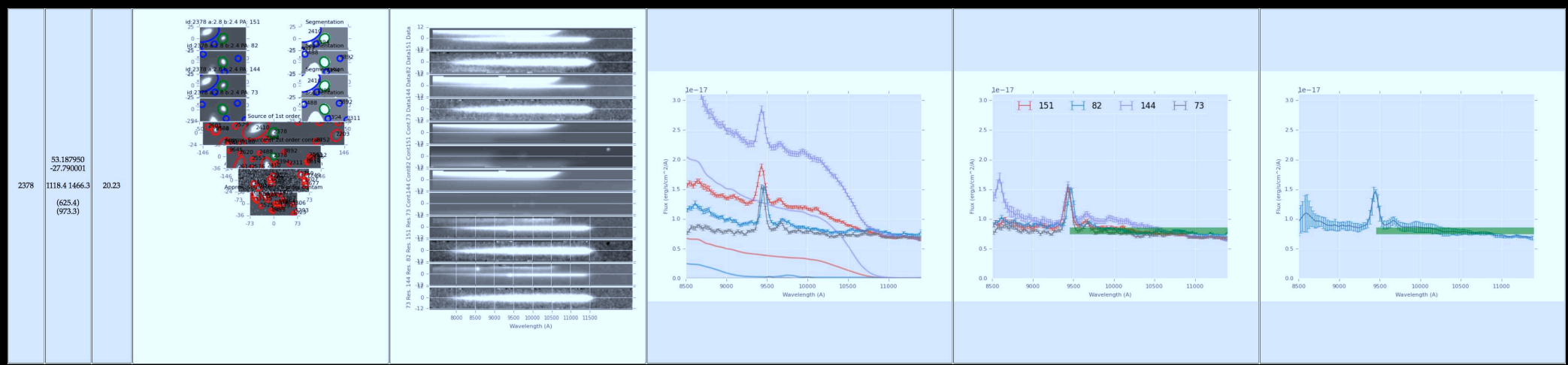
X-ray sources in GOODS-S1: FIGS ID + images + 2D & 1D spectra



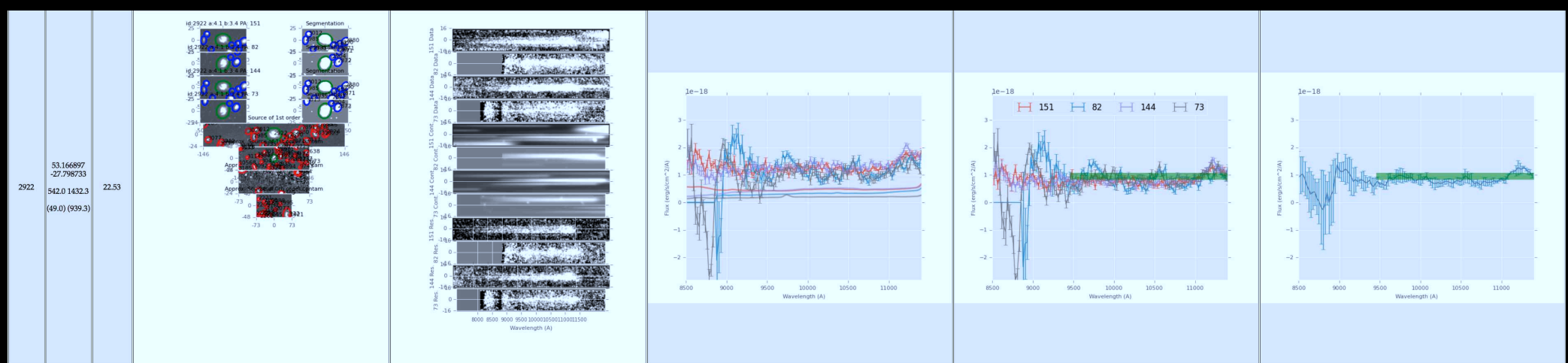
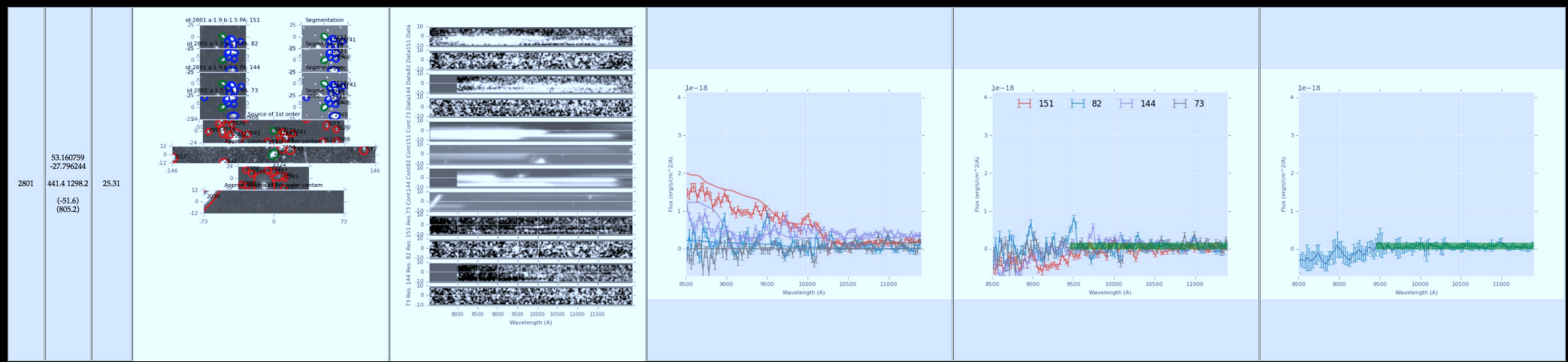
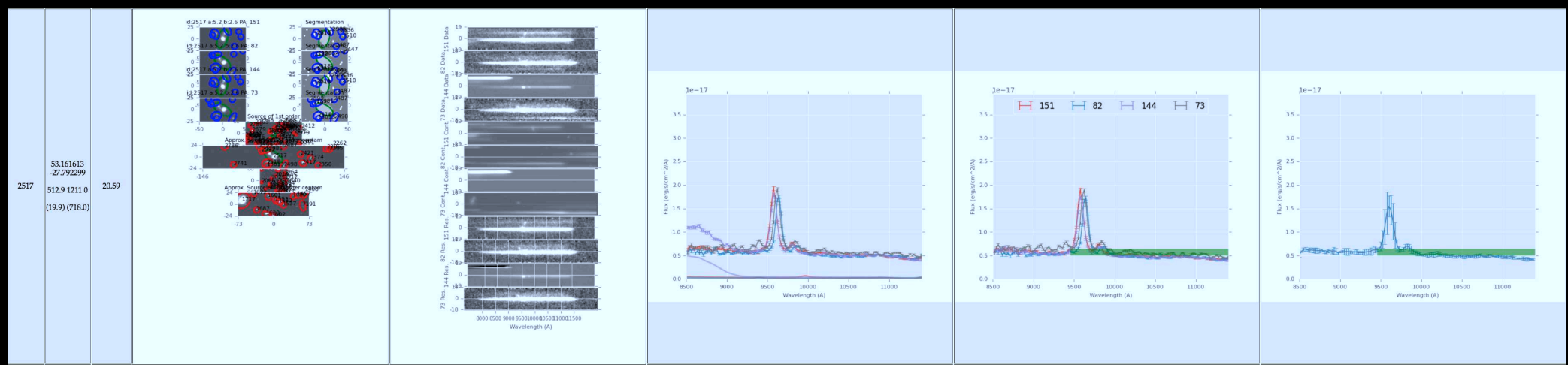
X-ray sources in GOODS-S1: FIGS ID + images + 2D & 1D spectra



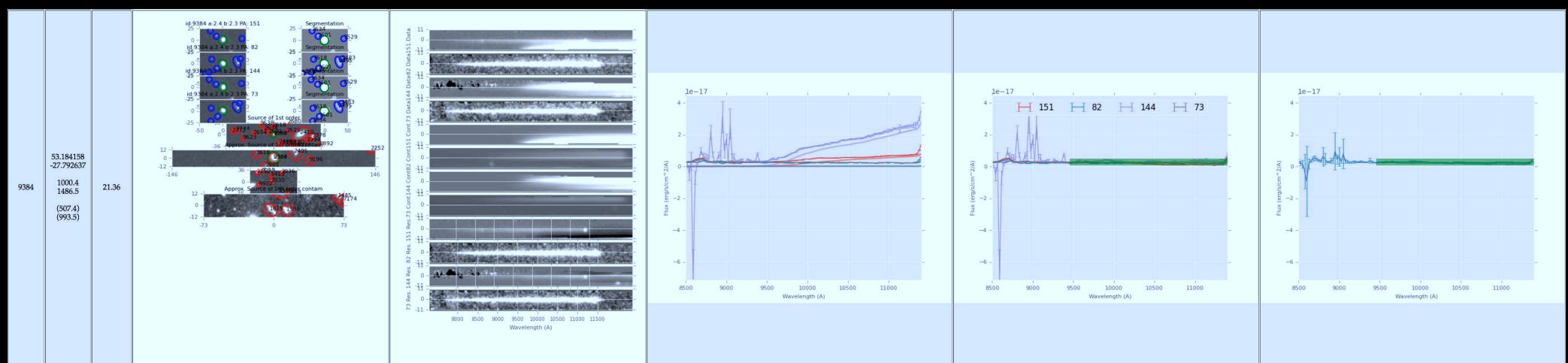
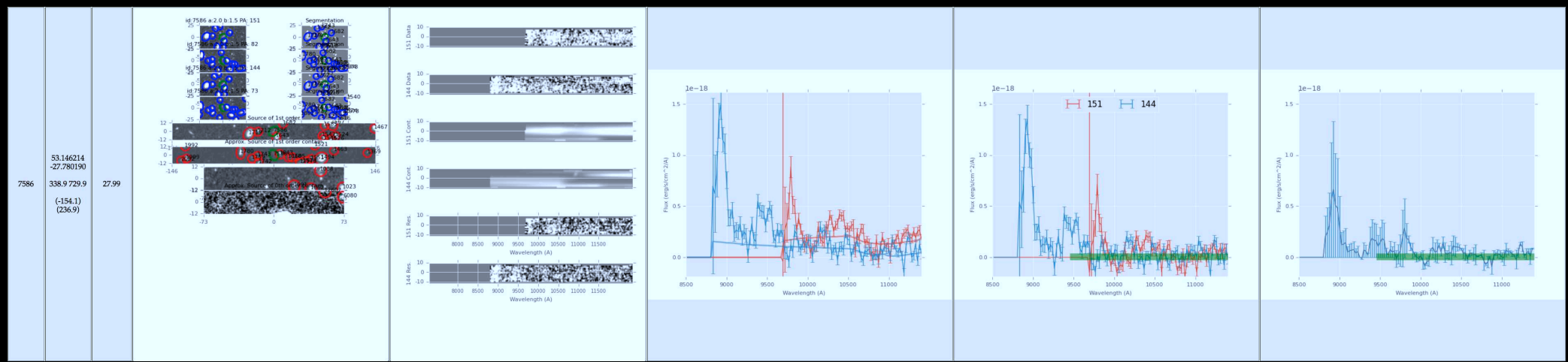
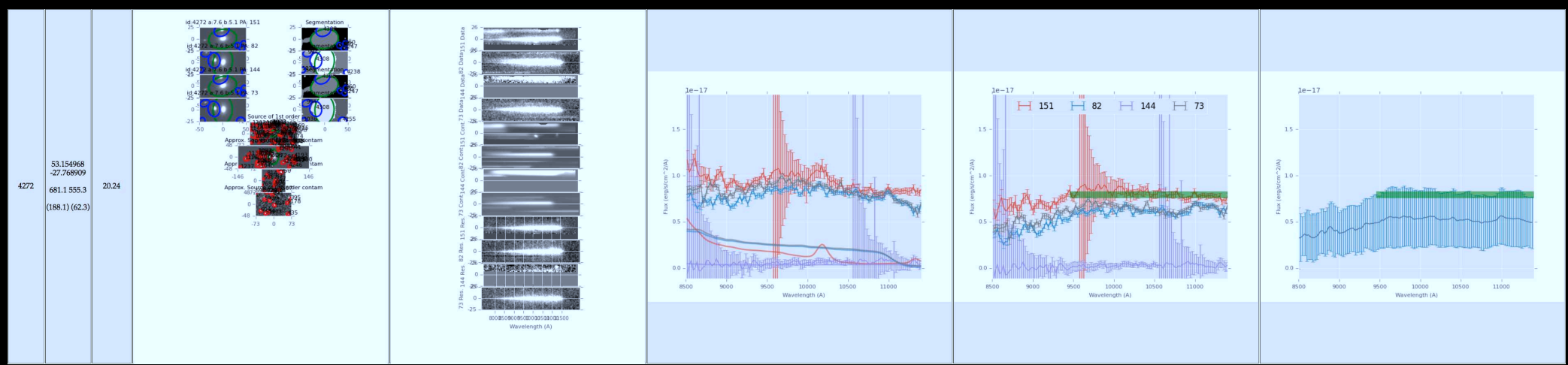
X-ray sources in GOODS-S1: FIGS ID + images + 2D & 1D spectra



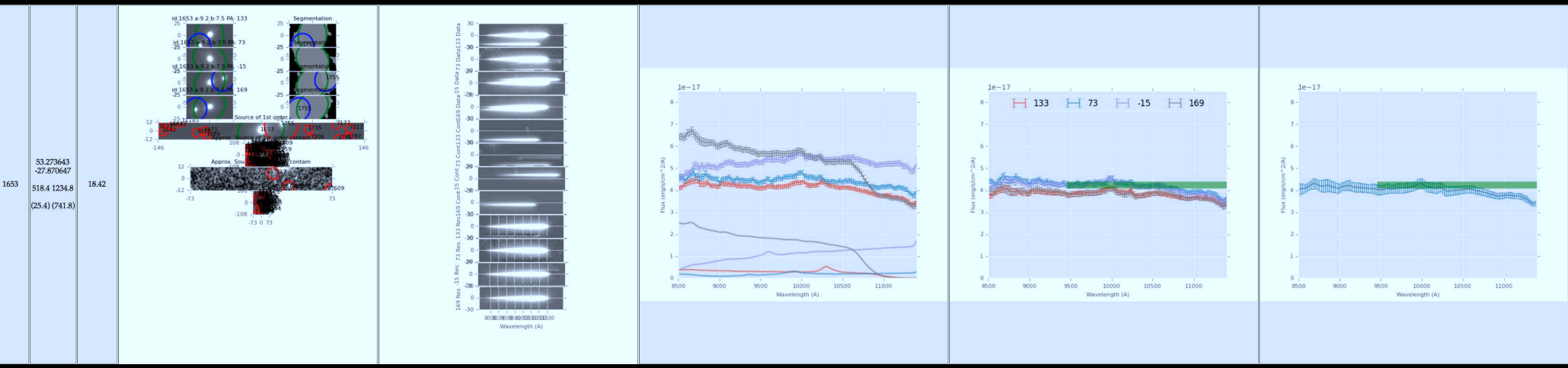
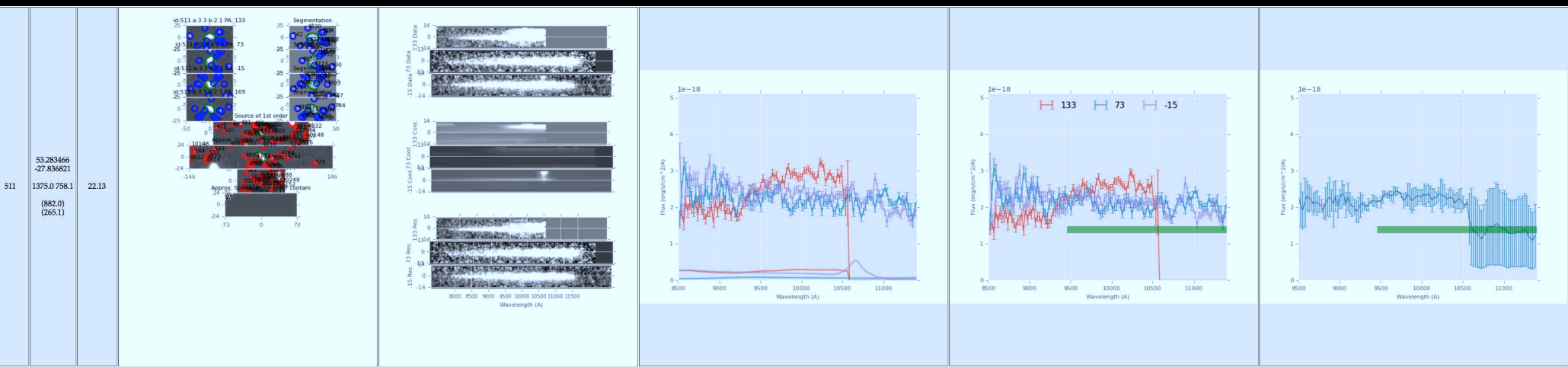
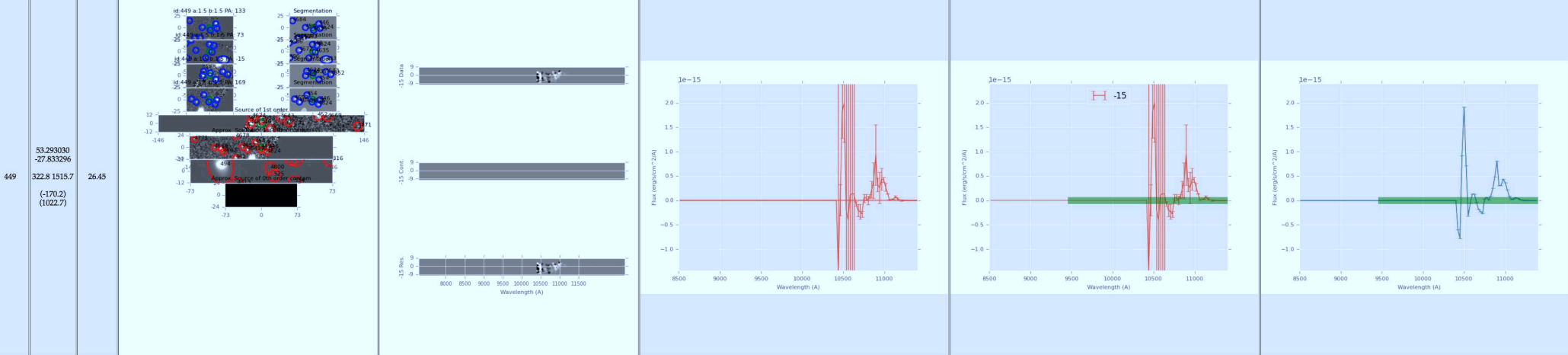
X-ray sources in GOODS-S1: FIGS ID + images + 2D & 1D spectra



X-ray sources in GOODS-S1: FIGS ID + images + 2D & 1D spectra



X-ray sources in GOODS-S1: FIGS ID + images + 2D & 1D spectra

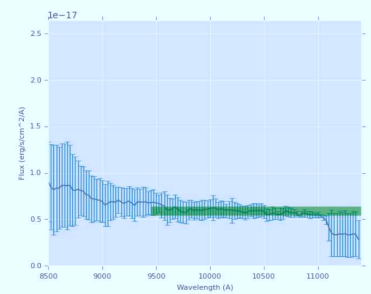
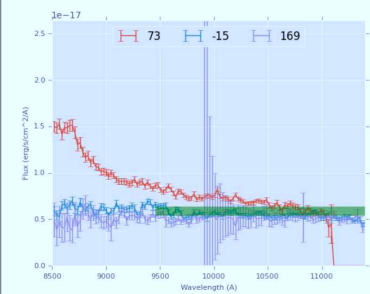
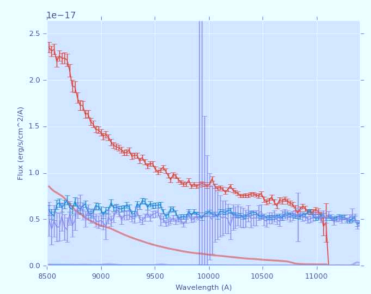
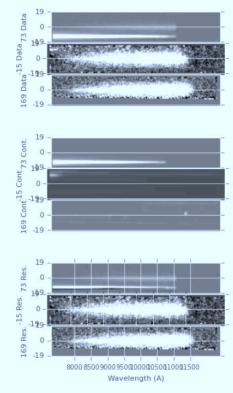
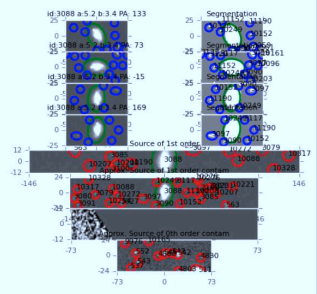


X-ray sources in GOODS-S2: FIGS ID + images + 2D & 1D spectra

3088

53.266083
-27.840584
(872.6)
(379.0)

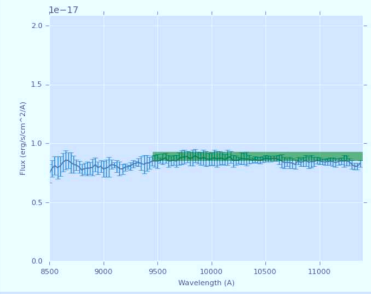
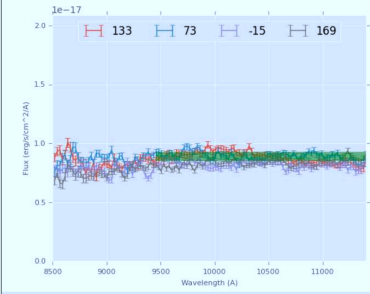
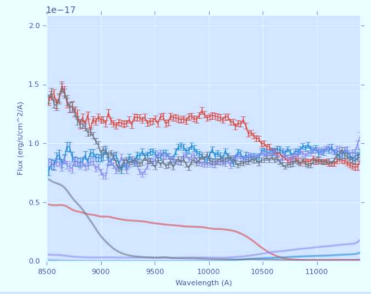
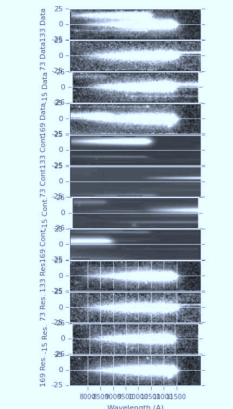
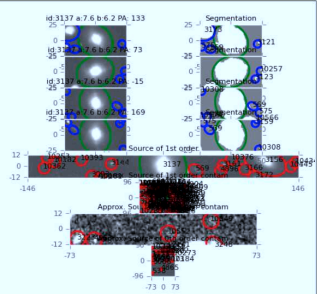
20.56



3137

53.284031
-27.842552
(774.9)
(386.0)

20.11



X-ray sources in GOODS-S2: FIGS ID + images + 2D & 1D spectra

(2) Radio, X-ray host SED-ages: trace AGN growth directly?

[1] DATA: HST GOODS BVizYJH photometry, VLT K-band + redshifts.

[2] METHOD: SED fitting for $0.12 \lesssim \lambda_{rest} \lesssim 1.6 \mu\text{m}$, using:

- (a) Bruzual-Charlot (2007) stellar population models.
- (b) + AGN power law $S_\nu \propto \nu^\alpha$ bluewards of the IR dust emission.
- VLT redshifts for all objects $AB \lesssim 24-25$ (Le Fèvre et al. 2004; Szokoly et al. 2004; Vanzella et al. 2005, 2008; see www.eso.org/science/goods/)

For typical $z \simeq 0.5-1.5$, BVizYJHK bracket the Balmer+4000Å breaks.

[3] SED fitting (for details, see Windhorst & Cohen 2010; WC10):

- Use solar metallicity and Salpeter IMF (most objects at $z \lesssim 2$).
- E-folding times τ in log spaced $n=16$ grid from 0.01-100 Gyr.
- $n=244$ ages \lesssim age of Universe at each redshift in WMAP-cosmology.
- Calzetti et al. dust extinction: $A_V = [0, 4.0]$ in 0.2 mag steps ($n=21$).
- $\alpha = [0, 1.5]$ in steps of 0.1 ($n=16$ values).

[4] Yields $\sim 10^6$ models for 1549 GOODS galaxies with VLT redshifts.

Best χ^2 fit stellar mass + possible AGN UV–optical power-law component.

Method follows WC10 and Windhorst et al. (1991, 1994, 1998), where HST + ground-based UBgrYJHK images showed non-negligible AGN components in mJy radio galaxies.

[5] Work to be done, including other potential caveats:

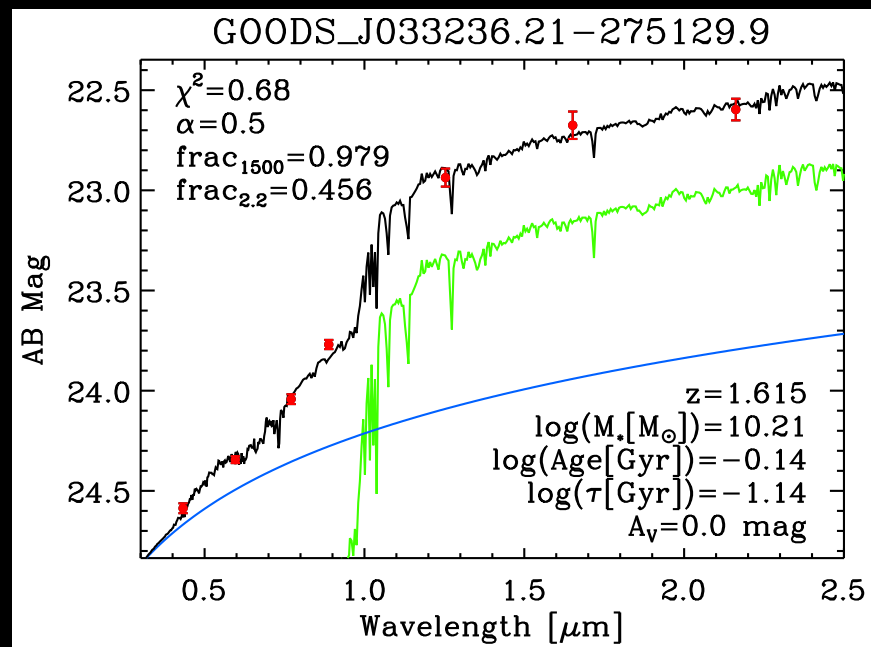
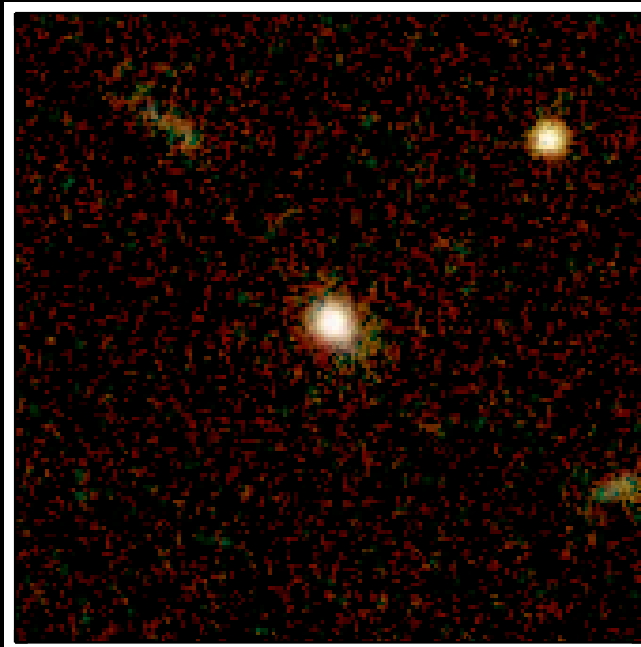
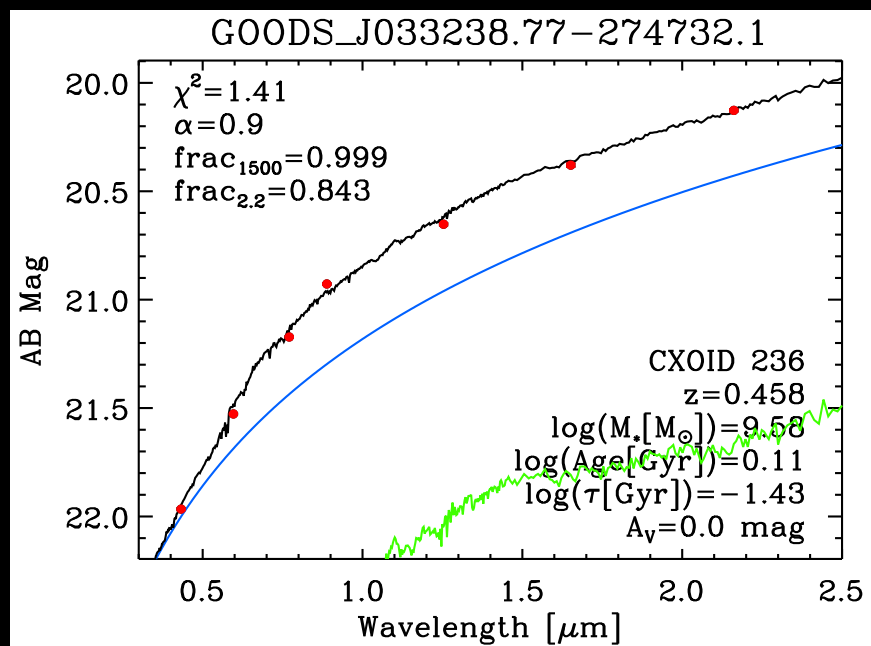
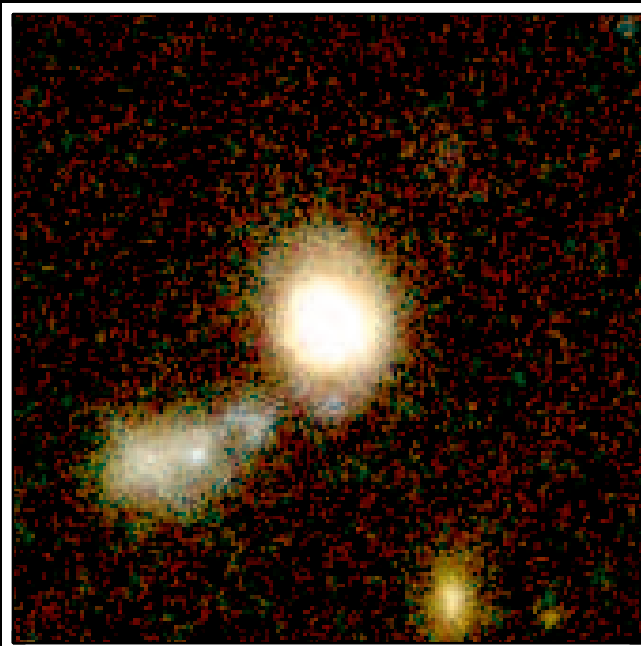
- Young stellar populations have power-law UV spectra (Hathi et al. 2008; Rutkowski et al. 2012, 2014), and may overestimate UV AGN power-law.

- Include IRAC data, and incorporate 1–2 Gyr red AGB population.

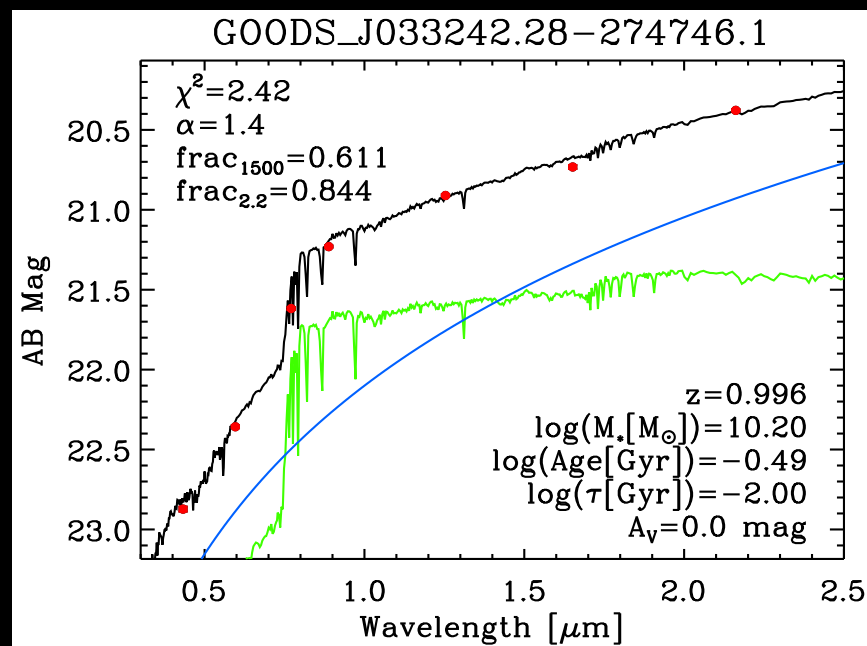
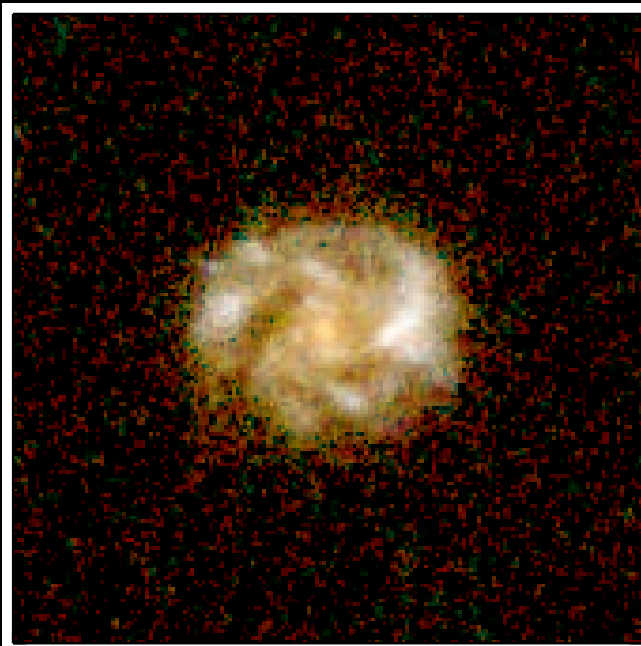
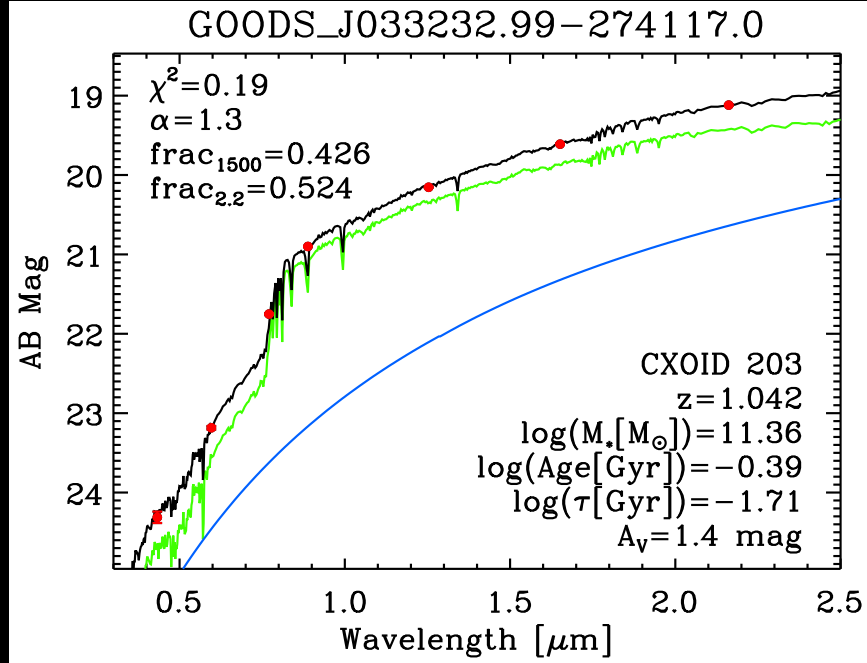
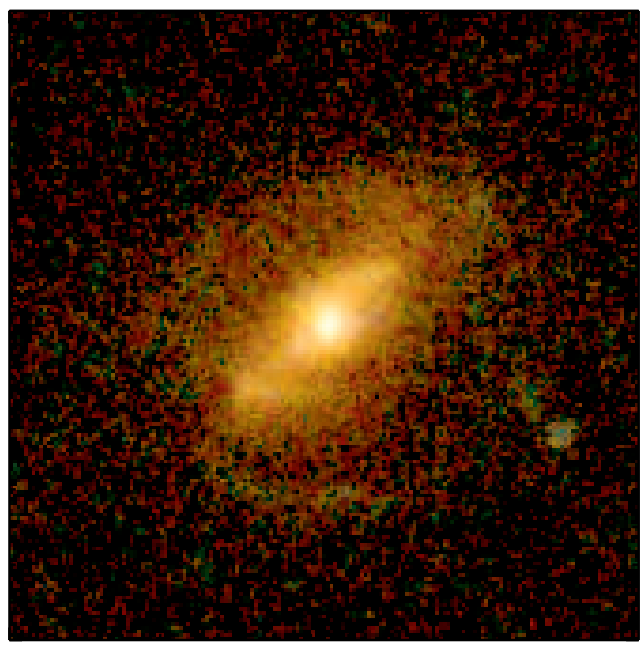
- Include GRAPES/PEARS+FIGS+3DHST spectra & fit with emission line templates, as needed.

[6] Repeat [1]–[5] for 7000 ERS objects with 10-band spz's to AB=27 mag.

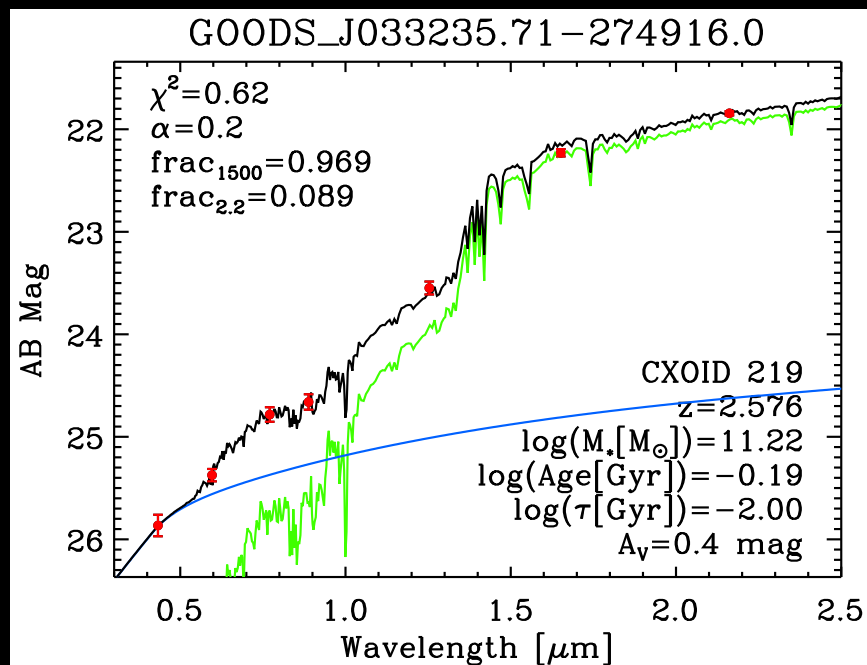
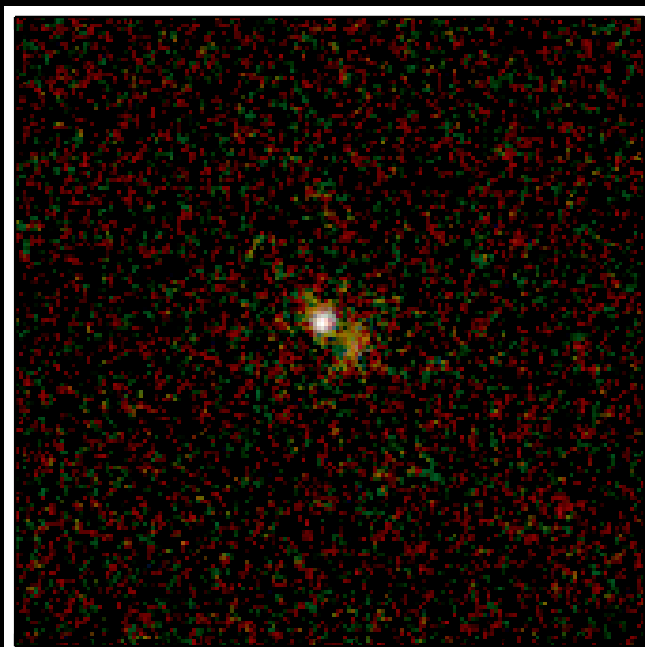
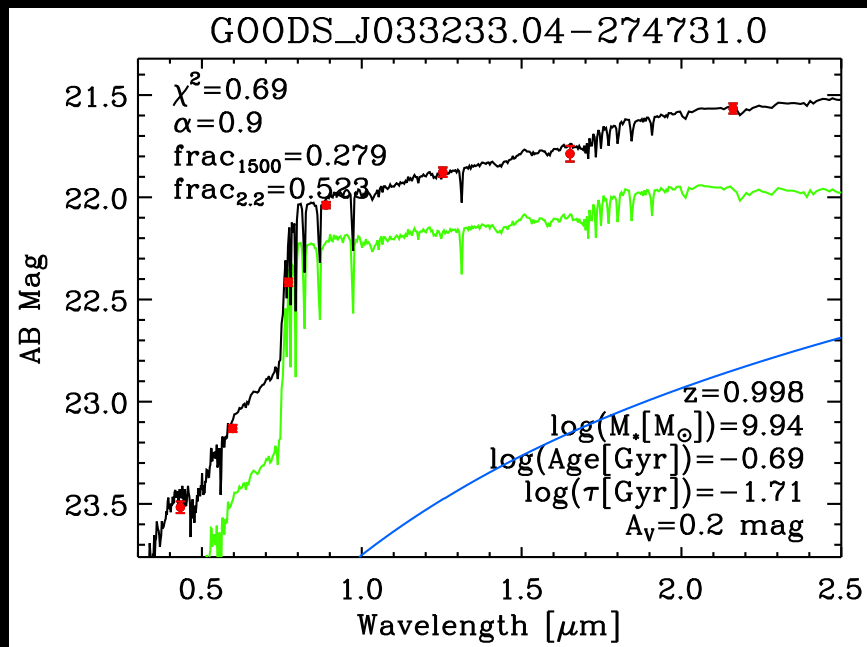
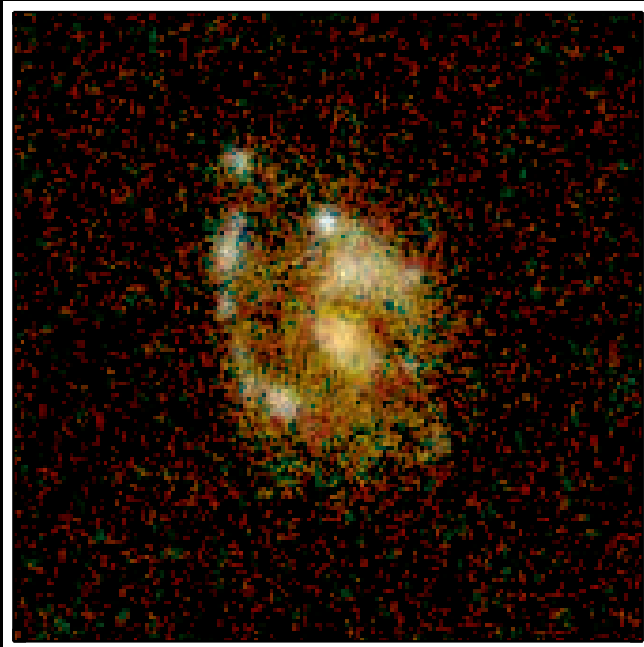
- Fit the BC03 stellar SED only to objects where χ^2 doesn't require both.



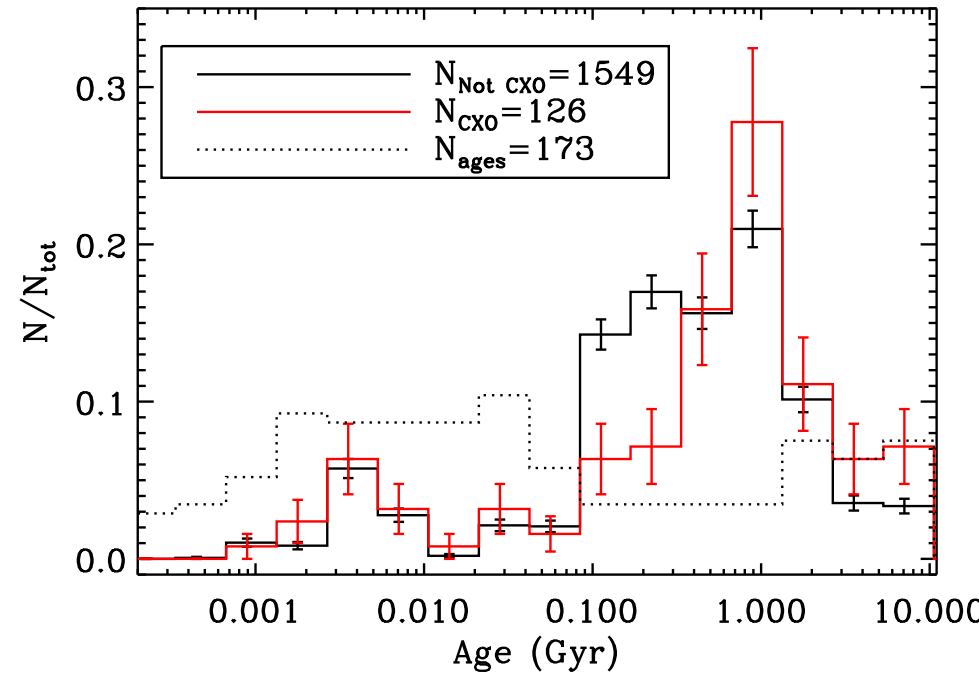
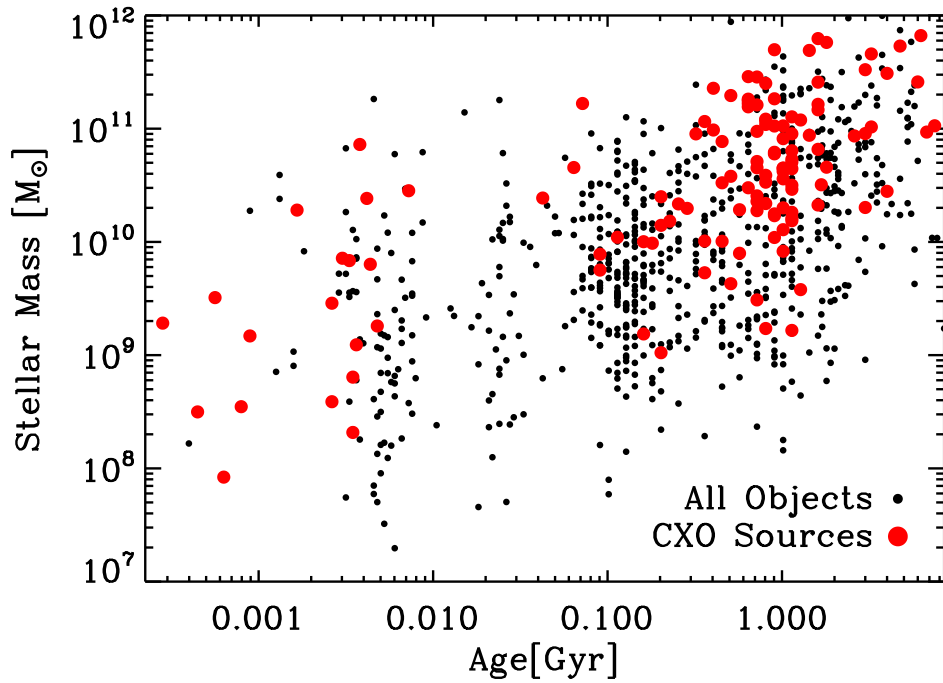
Windhorst & Cohen (2010): GOODS/VLT BVizJHK images
 Best fit Bruzual-Charlot (2007) SED + power law AGN.



Windhorst & Cohen (2010): GOODS/VLT BVizJHK images
 Best fit Bruzual-Charlot (2007) SED + power law AGN.



Windhorst & Cohen (2010; WC10): GOODS/VLT BVizJHK images
 Best fit Bruzual-Charlot (2007) SED + power law AGN.

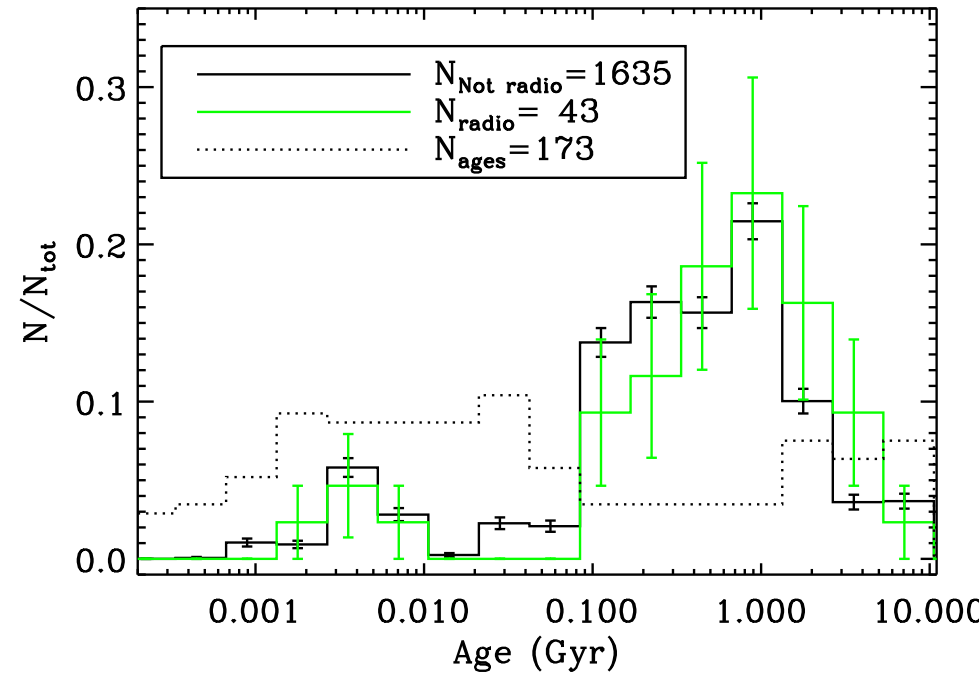
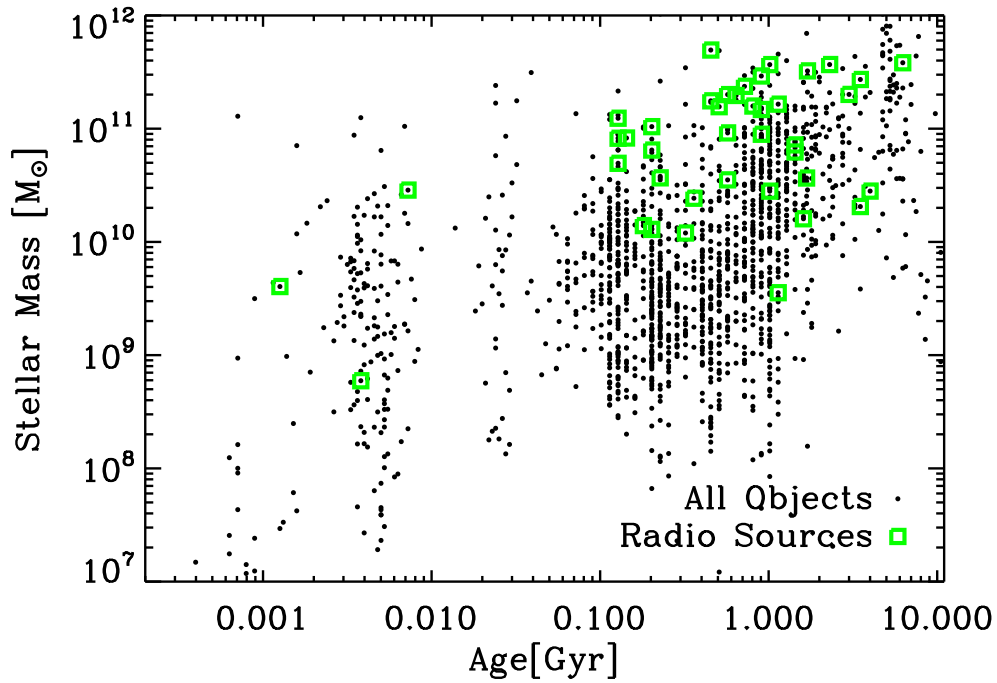


WC (2010): Best fit Stellar Mass vs. Age: X-ray and field galaxies.

Field galaxies have: Blue cloud of ~ 100 -200 Myr, Red cloud of $\gtrsim 1$ -2 Gyr.

- X-ray sources reside in galaxies that are a bit older than the general field population, but by no more than $\lesssim 0.5$ -1 Gyr on average.

- Include GRAPES/PEARS+FIGS+3DHST spectra & fit with emission line templates.

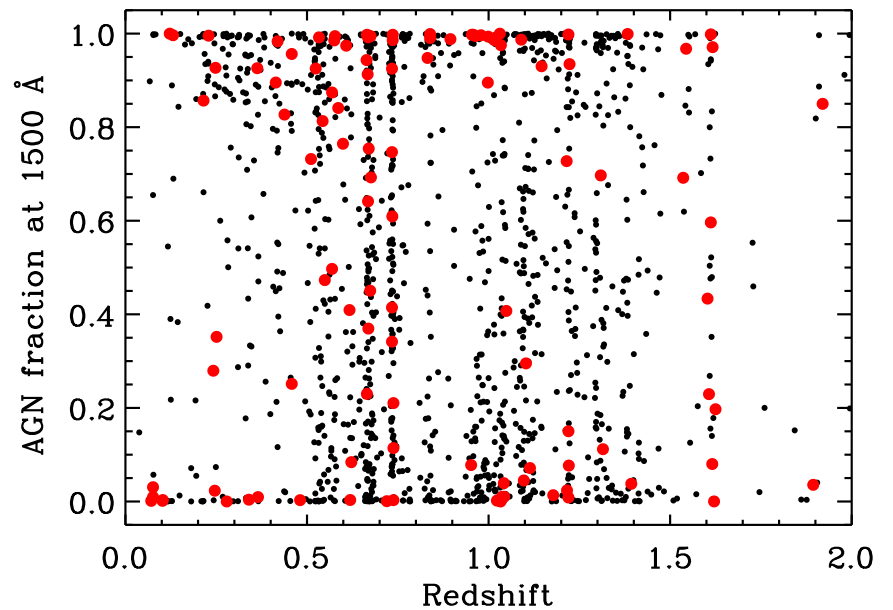
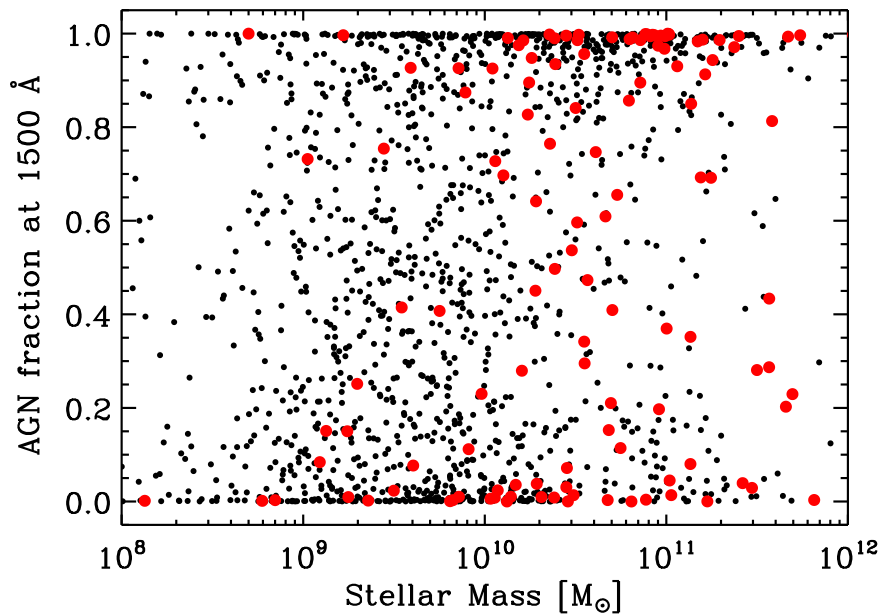
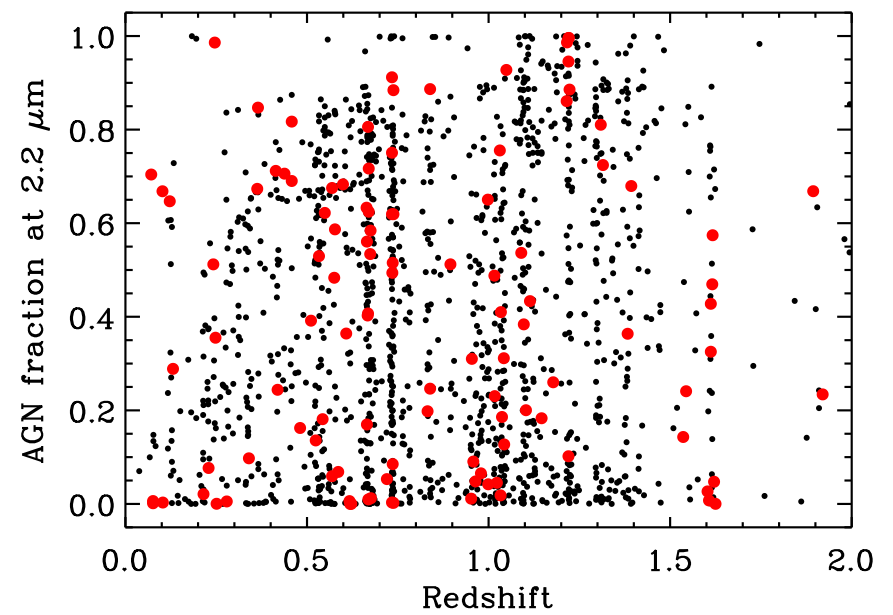
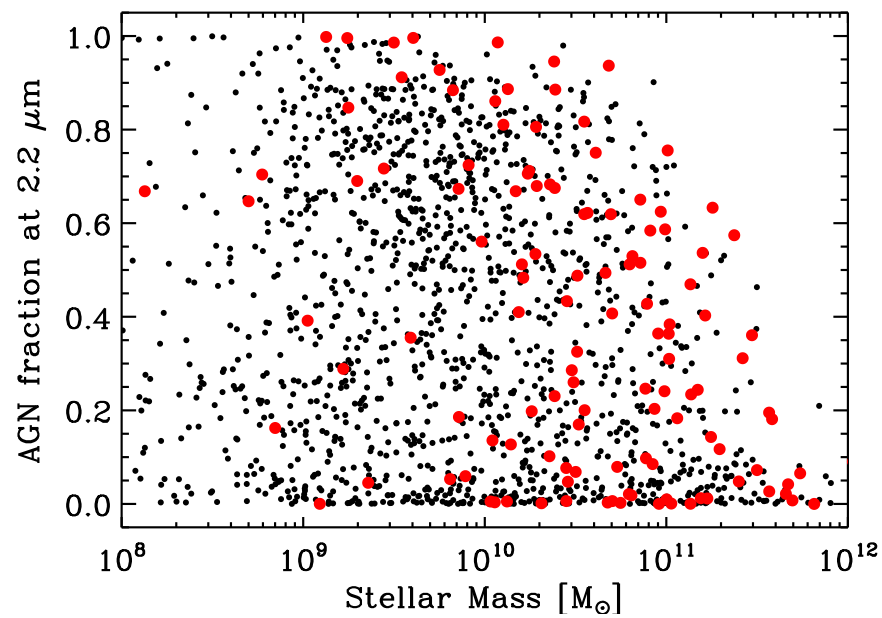


WC (2010): Best fit Stellar Mass vs. Age: Radio and field galaxies.

Field galaxies have: Blue cloud of $\sim 100\text{-}200$ Myr, Red cloud of $\gtrsim 1\text{-}2$ Gyr.

- Radio galaxies are (a bit) older than the general field population, but by no more than $\lesssim 0.5\text{-}1$ Gyr on average.

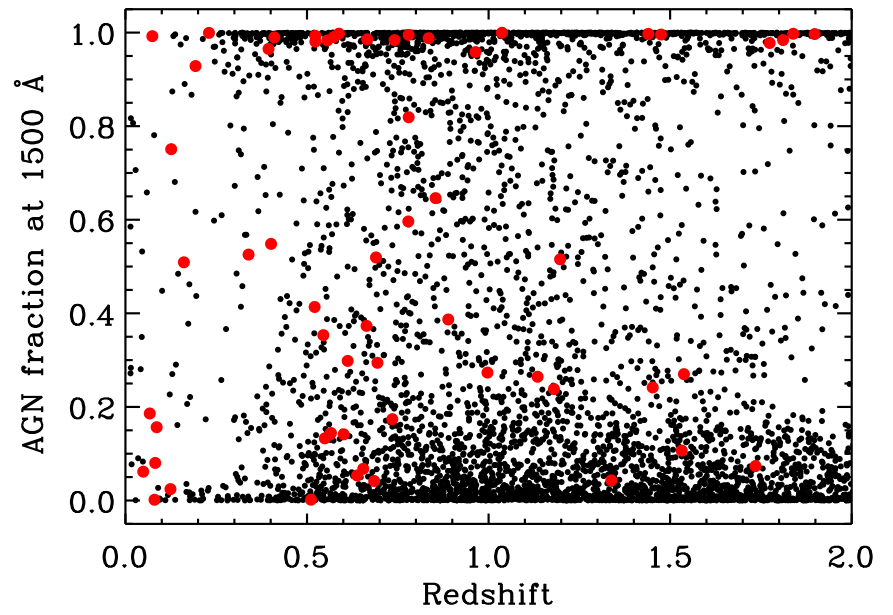
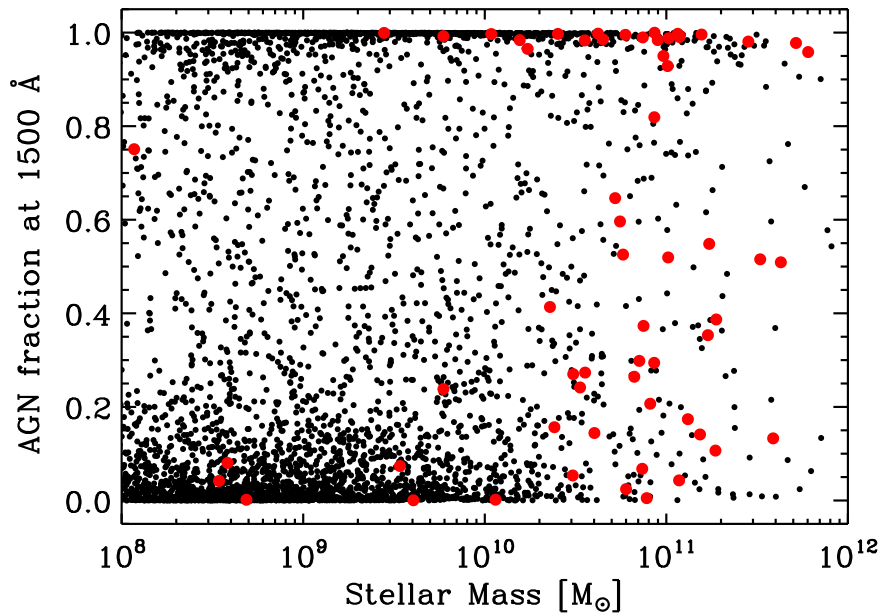
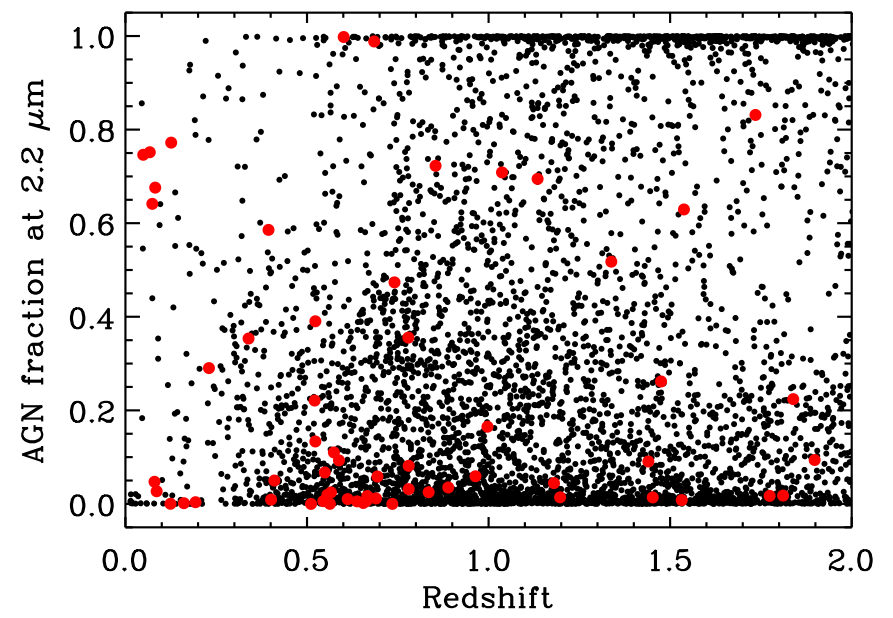
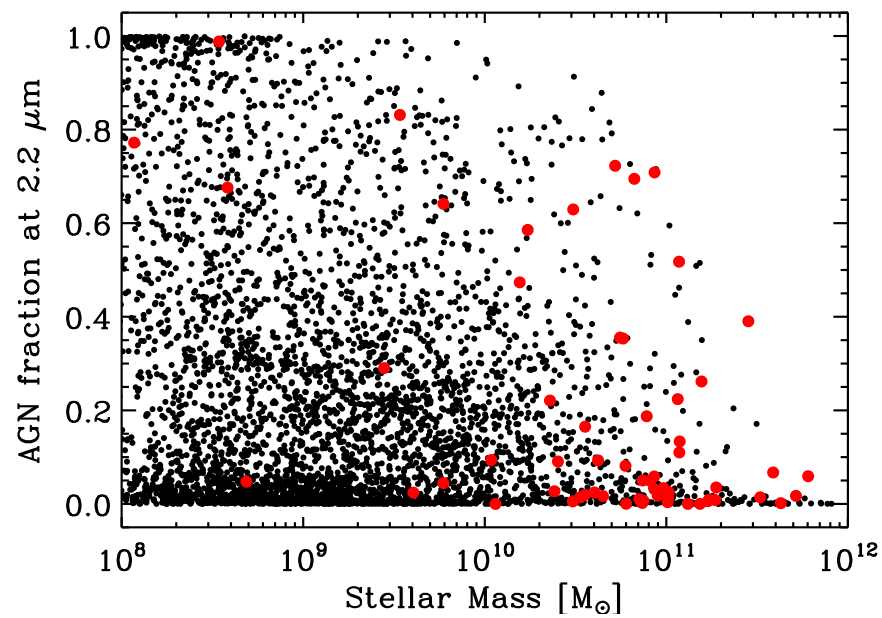
- Include GRAPES/PEARS+FIGS+3DHST spectra & fit with emission line templates.



WC (2010): AGN fraction vs. Stellar Mass & z : X-ray and field gxy's.

\Rightarrow Many more with best-fit $f(\text{AGN}) \gtrsim 50\%$ to be detected by IXO or SKA.

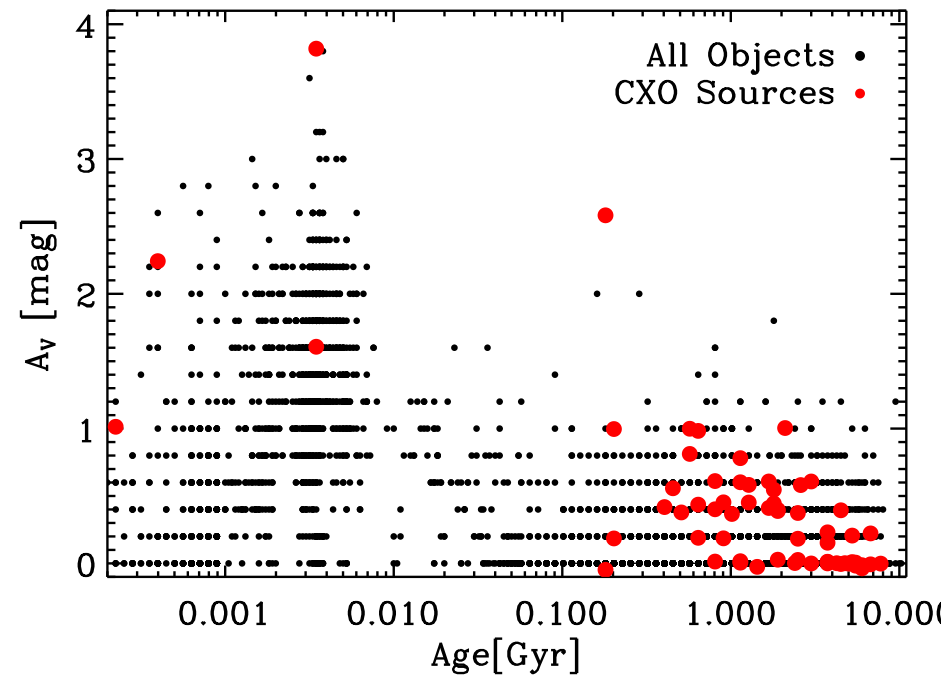
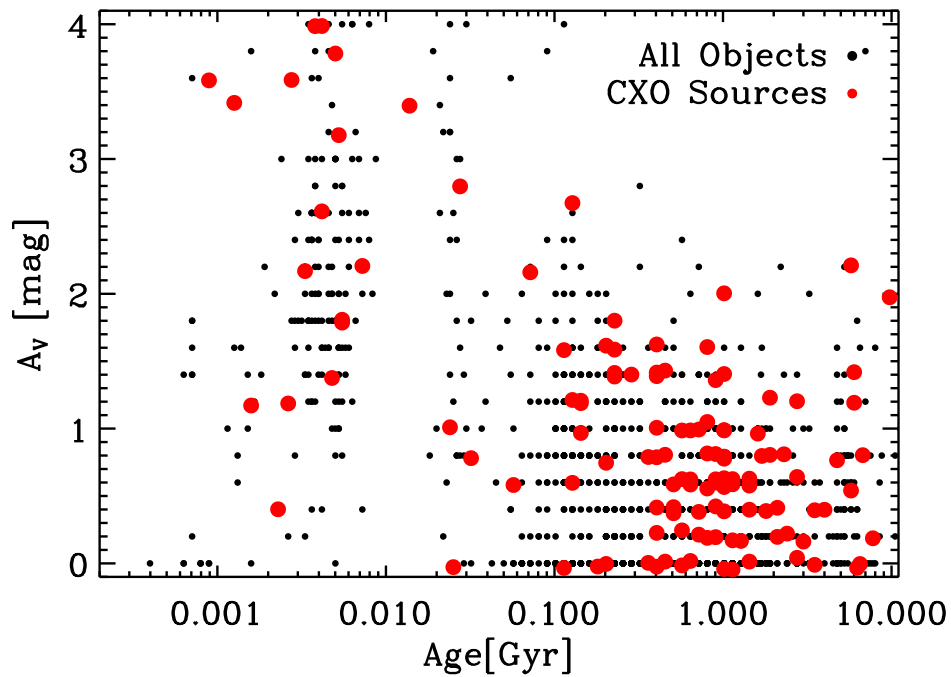
● Include GRAPES/PEARS+FIGS+3DHST spectra & fit with emission lines.



WC (2010): AGN frac vs. Stellar Mass & *spz*: X-ray & field gxys.

⇒ Many more with best-fit $f(\text{AGN}) \gtrsim 50\%$ to be detected by IXO or SKA.

● Include GRAPES/PEARS+FIGS+3DHST spectra & fit with emission lines.



LEFT: 1549 CDF-S objects with z 's. RIGHT: 7000 CDF-S ERS with spz 's.

WC (2010): Best fit extinction A_V distribution: X-ray and field.

- In Hopkins et al. (2006, ApJS, 163, 1) scenario, dust and gas are expelled *after* the starburst peaks and *before* before the AGN becomes visible.

- Older galaxies have less dust after merger/starburst/outflow.

- Age-metallicity relation may complicate this.

- Include GRAPES/PEARS+FIGS+3DHST spectra & fit with emission line templates, as needed.

(6) Summary and Conclusions

(1) Good FIGS spectra are available for about half of 36 faint radio sources and 53 faint X-ray sources inside GOODS-North+South.

(2) Emission lines seen in a fraction of these: weak AGN and post-starburst galaxies.

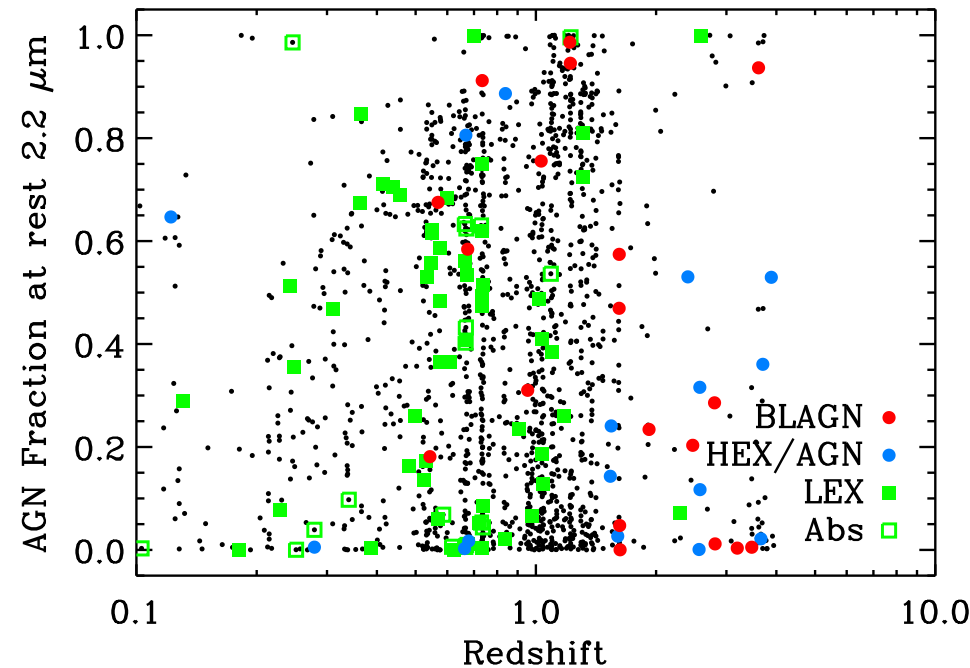
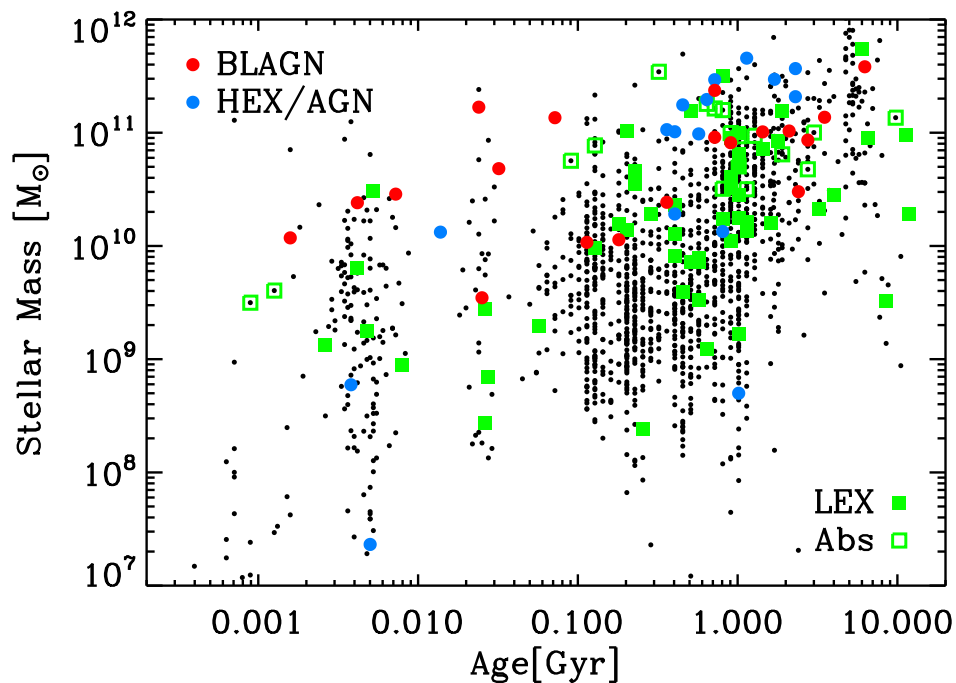
(3a) Need to sub-stack uncontaminated ORIENTS in FIGS spectra for cleaner results, and to enlarge usable sample.

(3b) Need to include GRAPES/PEARS+FIGS+3DHST spectra & fit with emission line templates, as needed.

(4) [TENTATIVE] Radio and X-ray selected galaxies at $z \simeq 0.5-2$ may on average be 0.5–1 Gyr older than typical LBG age of 0.1–0.2 Gyr.

(5) [TENTATIVE] AGN growth may stay in pace with Galaxy Assembly, but Radio &/or X-ray source may appear $\lesssim 1$ Gyr after merger/starburst.

SPARE CHARTS



WC (2010): At all ages, the most massive hosts are QSO-1/2's (based on AGN lines in *optical spectra* by Szokoly et al. 2004):

- This illustrates the well known L_X - L_{opt} correlation.

All optical AGN types: emission lines and absorption features.

Most $\gtrsim 0.5$ – 1 Gyr SEDs do not show AGN signatures in optical spectra.

- For majority of AGN-1's: $\lesssim 50\%$ of $2 \mu\text{m}$ -flux comes from the AGN ?

Many more with best-fit $f(\text{AGN}) \gtrsim 50\%$ to be detected by IXO or SKA.

- References and other sources of material shown:

<http://www.asu.edu/clas/hst/www/jwst/> [Talk, Movie, Java-tool]

<http://www.jwst.nasa.gov/> and <http://www.stsci.edu/jwst/>

Gardner, J. P., et al. 2006, Space Science Reviews, 123, 485

Mather, J., & Stockman, H. 2000, Proc. SPIE Vol. 4013, 2

Windhorst, R. A., et al. 1991, ApJ, 380, 36

Windhorst, R. A., Keel, W. C., & Pascarelle, S. M. 1998, ApJL, 494, 27

Windhorst, R. A. 2003, New Astron. Rev., 47, 357 “The MicroJansky and NanoJansky Population”

Windhorst, R. A., & Cohen, S. H. 2010, AIP Proc., 1291, 225 “How HST/WFC3 and JWST can Measure Galaxy Assembly and AGN Growth”

Windhorst, R. A., Cohen, S. H., Hathi, N. P., et al. 2011, ApJS, 193, 27